AN ABSTRACT OF THE THESIS OF

Muhammad Asif Soofi for the degree of Master of Science in Geophysics presented on August 5, 1991

Title: Crustal Structure of the Northwestern Continental Margin of the Indian Subcontinent from Gravity and Magnetic Data

Redacted for Privacy

Abstract approved: _____
Dr. Richard W. Couch

The continental margin off the coast of Pakistan between the Murray ridge and the Gulf of Cambay has been studied in this work using gravity, magnetic and bathymetric data. Two-dimensional gravity and magnetic models based on free-air gravity and residual magnetic data are developed along a north-south profile off the coast of Karachi. The purpose was to interpret the gross crustal structure of the region. A magnetic map has also been developed for the region between latitudes 20° N and 27° N and between longitude 60° E and 70° E.

The gravity model extends to a distance of about 1200 km seaward south of Karachi. The seaward end of the gravity model is constrained by seismic refraction data which suggest the presence of typical oceanic crust. The Moho depth at this end of the profile is about 12 km. At the landward end of the profile A-A' the Moho depth is not constrained by seismic data. The gravity

model suggests 27 to 17 km as the possible range of the depth of the Moho and a gradual thinning of the crust from land to sea. In addition, the gravity models as interpreted in this study show grabens at the distances of 350 and 450 km along the profile. If the graben-like structures are rift grabens formed during the rifting of India from Africa then transitional crust can be expected to extend to the 500 km mark along the profile A-A'.

Two dimensional models for the magnetic data along the profile were also developed. These anomalies can be interpreted as due to oceanic crust or magnetic bodies embedded in transitional crust. The possibility that the observed magnetic anomalies are due to oceanic crust has been studied in detail in this work. The location of the observed magnetic anomalies with respect to marine magnetic anomaly (28) observed earlier on the Indian Ocean floor, were compared to a marine magnetic time scale. To get a reasonable correlation between the observed and theoretical anomalies requires a considerable amount of adjustment in the spreading rate of individual magnetic blocks. Also on the magnetic map the trend of the lineation of these anomalies is perpendicular to the continental margin instead of being parallel to the continental margin as expected for a rifted continental margin. The presence of horst-and-graben structures in the inland region suggests the rifted nature for the continental margin off Karachi than the sheared nature. This indicates that the lineations should be parallel to the margin. But the magnetic lineations are perpendicular to the continental margin and if they are from oceanic crust then they would suggest that the margin is

a sheared margin, which contradicts the extensional structures observed inland. This makes it very unlikely that the source of these anomalies is oceanic crust. However, it is quite possible that the magnetic lineations observed in the map were parallel to the continental margin initially but later on the continent rotated clockwise along a fault landward of the magnetic lineation. This rotation is perhaps responsible for making the lineation perpendicular to the continental marign.

One objective of this study was to locate the continent-ocean boundary, but with the available amount of data it is not possible to decide on the most appropriate source for the observed magnetic anomalies. Hence it was not possible to decide exactly on the location of continent-ocean boundary. However, on the basis of gravity and magnetic data it can be said that the continent-ocean boundary lies at a distance of 500 km or greater along the profile.

# Crustal Structure of the Northwestern Continental Margin of the Indian Subcontinent from Gravity and Magnetic data

by

Muhammad Asif Soofi

A THESIS
submitted to
Oregon State University

in partial fulfillment of
the requirement for the
degree of

Master of Science

Completed August 5, 1991

Commencement June 1992

APPROVED:

Redacted for Privacy

Associate Professor of Geophysics in charge of major

Redacted for Privacy

Dean of College of Oceanography

Redacted for Privacy

Dean of Graduate School

Date thesis is presented August 5, 1991

Typed by the author Muhammad Asif Soofi

TABLE OF CONTENTS

LIST OF FIGURES

LIST OF APPENDIX FIGURES

# CRUSTAL STRUCTURE OF THE NORTHWESTERN CONTINENTAL MARGIN OF THE INDIAN SUBCONTINENT FROM GRAVITY AND MAGNETIC DATA

## INTRODUCTION

The Mesozoic breakup of Gondwanaland resulted in the movement of it's broken landmasses in different directions. India started drifting from Gondwanaland in mid-Jurassic time at the spreading rate of 3 to 5 cm/year (Biswas, 1982; Powell, 1979). The spreading rate reached 15 to 20 cm/year in late Cretaceous time (Powell, 1979). During the drifting phase that occured during Mesozoic time India rotated counterclockwise by about 50° (Klootwijk, 1979). The spreading rate slowed down in Eocene time after collision with island arcs (Powell, 1979; Klootwijk, 1979). Continental collision between Eurasia and India began in Eocene to Oligocene time. Since that time India has moved slowly into Eurasia forming the Himalaya and the associated mountain ranges (Biswas, 1982; Powell, 1979) (FIG. 1).

The Himalayan orogenic belt forms the northern part of the collision zone between Eurasia and India. This collision zone extends southward along the Ornatch-Nal/Chaman fault (FIG.1). Gravity studies in the Sulaiman and Salt Range region along the Ornatch-Nal/Chaman fault (FIG. 1) have shown that the rifted continental margin of the subcontinent is at different phases of

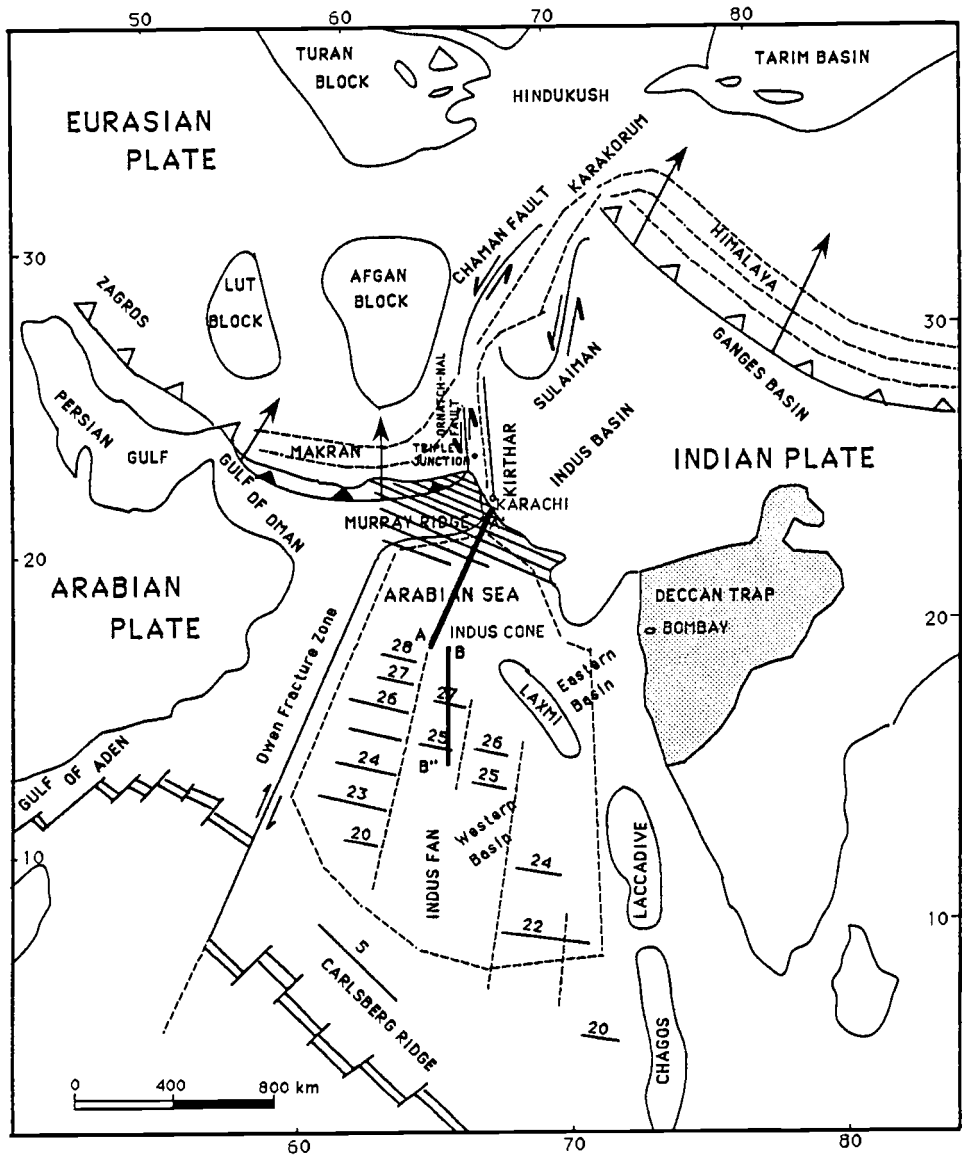


FIG.1 General tectonic map of the northwest Indian Ocean and the surrounding continental masses. Hachured area indicates the area for which a magnetic map has been developed. Arrows indicate the direction of plate motion. A-A' and B-B" are the profiles along which crustal models are developed. (Modified from Kolla and Coumes, 1987; Lut, Afgan and Turan blocks and Tarim basins are included from Powell, 1979).

destruction along this fault (Jadoon et al., 1991; Khurshid et al., 1990). Gravity models of continents colliding under Airy isostatic equilibrium and no erosion, which reveal the variation in Bouguer anomaly under different stages of continental collision (Lillie, 1991), support the hypothesis that from south to north along the northwest boundary of the Indian plate the paleo-passive continental margin of India is in an increasing stage of convergence.

Raza et al. (1990) have reported horst-and-graben structures in the southern region of the Indus basin (FIG. 2). The Pano Aquil rift graben in the southern Indus basin is enclosed by the Mari horst in the north and Jaccobabad-Khairpur horst in the south (Raza et al., 1990). These structures formed during the rifting of the Cambay basin in late Cretaceous time and were later modified by fold belts and depressions which formed as a result of lateral gliding of the Indian plate into the Eurasian plate ( Raza et al., 1990). Also, Kazmi (1979) and Quittmeyer et al. (1979) have reported a 16 June, 1819 earthquake of east-west strike parallel to the mapped fault along the southern boundary of India and inland of the coastline in the Rann of Kutch (FIG. 1 & 3 ). The movement along the fault was dip-slip, down-to-the-south.

The area of this study lies offshore to the south of the Ornatch Nal-Chaman fault and southern Indus basin extending to 700 km seaward in the Arabian Sea (FIG. 2). The objective of this study is to get a general picture of the crustal structure of this continental margin off Pakistan. The structure of the crust

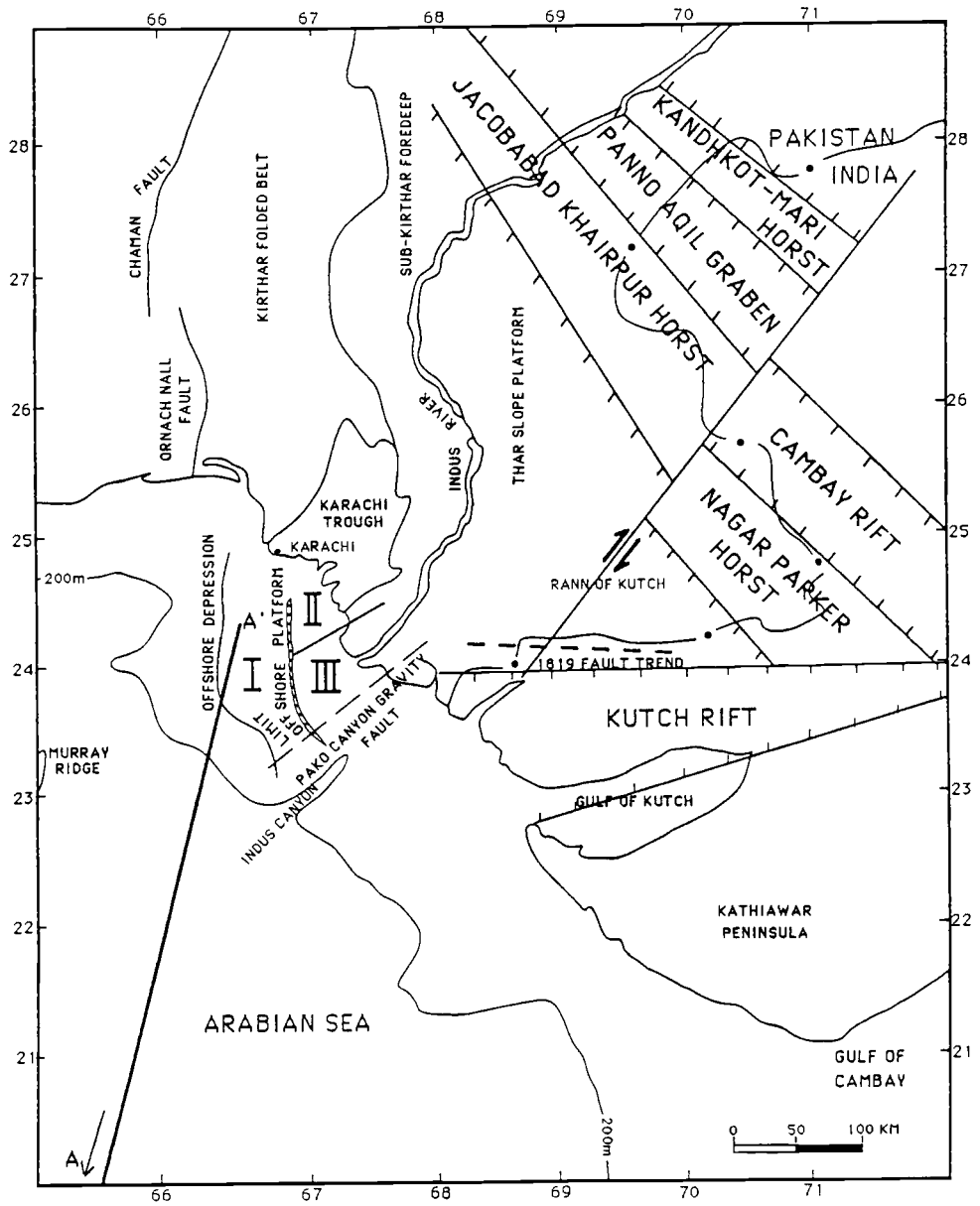


FIG.2 Map of the southern and offshore Indus basins. The tectonic divisions of the offshore basin are (Shuaib, 1982): I, offshore depression; II, trough platform; and III, Thar platform or deltaic area. The Pako Canyon gravity fault marks the eastern limit of the offshore Thar platform. Also shown is the fault trend of an 1819 earthquake from Kazmi (1979). Horst-and-graben structures are from Raza et al. (1990). (Modified from Quadri and Shuaib, 1986).

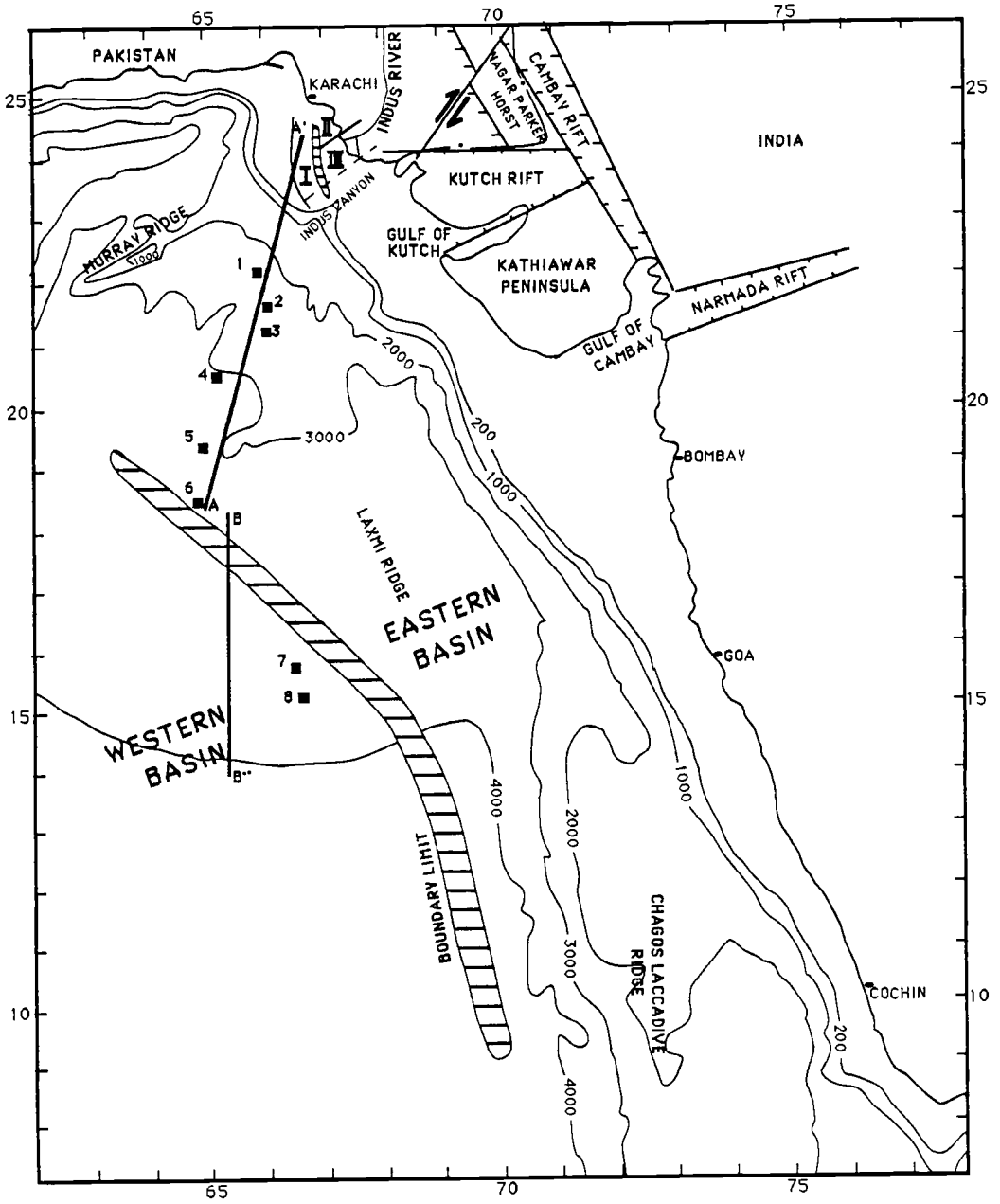


FIG.3 Map of the western continental margin of the Indian subcontinent. A-A' is the profile used for gravity and magnetic modeling. Numbers 1, 2, 3, and 4 are sonobuoy stations from Naini and Talwani (1983). I, II and III are described in FIG.2. Striped area marks the ridges and separates the western and eastern basins. Rift basins and horst structures are from Raza et al. (1990). (Map modified from Naini and Talwani, 1983).

observed in this continental margin will give an idea about the crustal structure beneath the Ornatch-Nal/Chaman fault.

The problems addressed in this thesis for the continental margin off Karachi are: (i) the location of the continent-ocean boundary, (ii) the width of the zone of transition from continental crust to normal-thickness oceanic crust, (iii) the nature of the oceanic crust adjacent to the continental margin, and (iv) the variation in the depth of the moho from continent to ocean. Changes in thickness of the continental crust give clues to the extent of crustal extension of the continental margin during rifting.

To address the above mentioned problems for the continental margin south of Karachi crustal models based on gravity and magnetic data have been developed. Also a magnetic map for the area extending from 60° to 70° E and 20° to 27° N has been prepared to assist the interpretation.

# GEOLOGY AND TECTONICS

The tectonic framework of the Arabian Sea and the adjacent northern Indian Ocean is a combination of divergent, transform, and convergent boundaries and a triple junction. The Carlsberg ridge is the spreading center along which new oceanic crust of the Indian Ocean is forming. The ridge extends northwest and terminates in the Owen fracture zone (Jacob and Quittmeyer, 1979) (FIG. 1). The Owen fracture zone is a transform boundary between the Arabian and Indian plates. It extends northward and connects to the Ornatch Nal/Chaman fault through the Murray ridge (FIG. 2). The Murray ridge and Owen fracture zone are the features along which right-lateral strike-slip motion is occuring between the Indian and Arabian plates (Jacob and Quittmeyer, 1979). The Murray ridge separates the continental margin of the Indus offshore basin from the active subducting continental margin of the Makran region (FIG. 1).

The Ornatch Nal/Chaman fault separates the Indian plate to the east from the Eurasian plate to the west (Kolla and Coumes, 1987) (FIG. 1). It also connects the Makran convergence zone to the south with the Himalayan convergence zone to the north (Jacob and Quittmeyer, 1979). Seismicity suggests left-lateral, strike-slip motion along this fault (Quittmeyer et al., 1979). Near Karachi, the Makran convergence zone, Murray ridge and the Ornatch Nal/Chaman fault form a triple junction of the type FFT (transform fault, transform fault and trench) of McKenzie and

Morgan (1969). At the Makran convergence zone the Arabian plate is subducting beneath the Lut and Afghan microplates (Jacob and Quittmeyer, 1979). The Himalayan convergence zone is the northern boundary of the Indian plate where the Indian plate is subducting beneath Eurasia (Duroy, 1989; Malinconico, 1989) (FIG. 1).

Ophiolites have been observed along the Ornatch Nal/Chaman fault (Farah et al., 1982; Powell, 1979) and in the Himalayan region (Powell, 1979). These ophiolites are pieces of oceanic crust obducted by convergence along the Chaman fault (Farah et al., 1982). Recent studies (Jadoon et al., 1991; Khurshid, 1990) suggest subduction of the Indian plate beneath the Eurasian plate along this fault.

In the northern section of the west Indian continental margin, which is west of my study area, there are the Cambay, Kutch and Narmada basins (FIG. 2 & 3). In the land region to the north of my research area is the Indus basin (Raza et al., 1990) (FIG. 2 & 3). The crustal setting of these basins is in the form of horst-and-graben structures (Raza et al., 1990; Naini and Talwani, 1983; Chowdry, 1975; Raju, 1968). This suggests that they have formed during rifting of the Indian sub-continent. Similar types of structures have been observed in a study of the eastern United States continental margin by Klitgord and Grow (1980), Klitgord and Behrendt (1979) and Folger et al. (1979).

A geological section for the Kirthar region, which is located in the southern Indus basin, has been constructed by Raza et al. (1989) on the basis of seismic data. This section shows faulting

through Jurassic time. This interpretation suggests the pre-rift sediments to be older than Jurassic in age. The onset of seafloor spreading started during marine magnetic anomaly 28 (63 Ma) (Naini & Talwani, 1983) however, because there is a large gap between anomaly 28 and the continental shelf off Karachi the seafloor spreading might have started earlier than 63 Ma. The syn-rift sediments appear to span Jurassic to late-Cretaceous time and so the post-rift sediments are Paleocene to Recent in age.

Physiographically, the Indus offshore basin has been divided into three parts: (I) the offshore depression in the west between the Murray ridge and the continental margin hinge line at roughly 67° longitude; (II) the offshore Karachi trough platform in the middle between the hinge line and the Karachi trough shore line; and (III) the Thar slope offshore platform or the Indus River deltaic area in the east (Shuaib, 1982) (Fig.2).

Shuaib (1982) has reported nine wells drilled in the offshore and onshore Indus basin. The maximum depth of 4335.0 meters was attained by the well Dabbo Creek-1 drilled on the onshore platform. These wells have penetrated up to Cretaceous age strata and only in the offshore platform region. The study of these wells suggests that the syn-rift sediments of Cretaceous age observed in the offshore platform are thicker toward the coast than toward the ocean. Also, the post-rift sediments of Paleogene age occur more on the onshore than on the offshore platform which is perhaps due to regression of the sea at that time. This regression of the sea didn't allow much sediment to reach the present offshore area. The Neogene sediments are however almost absent

in the onshore and offshore platform but they are present in the offshore depression.

To the southeast of Karachi, the Indus River discharges into the Arabian Sea forming the deep submarine Indus canyon (FIG.2) (Naini and Talwani, 1983). The Indus canyon and the numerous channels associated with it have been formed by the discharge of sediment-laden Indus waters (Naini and Talwani, 1983). Sediments transported through these channels and the Indus canyon to the Indian Ocean formed a terrain of rough topography known as the Indus cone (FIG.1) (Naini and Talwani, 1983). The Indus fan (FIG.1) is a prominent feature of the northwest Arabian Sea spreading over an area of $1.1X10^6$ $km^2$ with a maximum thickness of sediment of approximately 10 km near the continental margin (Kolla and Coumes, 1987).

The width of the continental shelf at the southern end of the western continental margin of India is about 50 to 60 km (FIG. 3). The shelf gradually increases in width northward and is widest north of the Bombay offshore basin where it attains a width of about 300 km. This widening of the shelf has been attributed to numerous extensional faults, which have given rise to a series of narrow linear horst-and-graben structures which are typical features of passive continental margins (Biswas, 1982). Recent studies by Gopala Rao (1990) using magnetic data delineates faults and rift-related structures in the Bombay offshore basin.

The western continental shelf of India has a large carbonate bank in the form of the Bombay offshore basin. Seaward the

carbonates grade into clastic sediments in the basins of Kutch, Cambay and Narmada (Biswas, 1982). These basins are underlain by seaward-diverging fault-bounded grabens (Biswas, 1982). On the basis of study of these basins Biswas (1982) has suggested that the rifting of the western continental margin of India occured from north to south. The Kutch basin formed in early Jurassic time, the Cambay basin in early Cretaceous time and the Narmada basin in late Cretaceous time. These different rifting events occured during northward migration of the Indian plate relative to Africa (Biswas, 1982).

The Laxmi and Laccadive-Chagos ridges are important features on the floor of the Indian Ocean (FIG. 3). The composite ridge extends a distance of 2200 km in a north-south direction from the Laccadive Islands at $14^{o}$ N to the Chagos Islands at $6^{o}$ S (Naini and Talwani, 1983). The ridges bend concavely to the west. These ridges divide the northeastern Arabian Sea into two basins. The eastern basin and the western basin (Naini and Talwani, 1983). The eastern basin crust is transitional in nature with a thickness more than that of normal oceanic crust while the western basin evolved by the process of sea floor spreading and is underlain by oceanic crust (Naini and Talwani, 1983; Naini, 1980). The crustal thickness of the Laxmi ridge is greater than 20 km and it may be continental in origin (Naini and Talwani, 1983). The Chagos-Laccadive ridge is similar in structure to the Laxmi ridge and a continental origin has been suggested for it, too (Naini, 1980).

# PREVIOUS GEOPHYSICAL WORK

Bathymetry, gravity, magnetic and seismic reflection data for the northwest Arabian Sea and the northern Indian Ocean recorded during the Indian Ocean Expedition (Udintsev, 1975; Admiralty, 1963) were collected. Until now, however, geological interpretations have been presented only for a part of the northeastern Arabian Sea (Naini and Talwani, 1983; Naini, 1980).

## Bathymetry

Detailed bathymetric and physiographic maps of the Indian Ocean and associated seas were prepared during the International Indian Ocean Expedition (Heezen and Tharp, 1966). These maps delineate the major tectonic structures of the western Indian continental margin and the adjacent Arabian Sea. The general interpretation of the maps suggests that the northwest continental margin of the Indian subcontinent has a wide continental shelf and a submarine canyon that runs through this continental margin into the deep ocean. The maps show a smooth gradient of the bathymetry of the Indus fan over the abyssal plain. The western basin ranges in depth from 3.4 to 4.3 km and has an average depth of 3.8 km. The eastern basin is shallower than the western basin with depths varying from 1.8 to 4.3 km and has an average depth of 3.2 km (Naini and Talwani, 1983). The western basin has

normal-thickness oceanic crust, whereas the eastern basin has extended continental crust of thickness less than normal thickness continental crust (Naini and Talwani, 1983).

## Gravity

Free-air and Airy isostatic gravity anomaly maps of the region have been prepared by Naini and Talwani (1983). The depth of compensation used for the isostatic gravity anomaly map is 30 km and the density contrasts are 1.6 $gm/cm^3$ across the crust-water interface and 0.5 $gm/cm^3$ across the crust-mantle interface. The free-air gravity anomaly map (25 mgal contour interval) shows regional negative free-air gravity anomalies. The map shows a linear belt of positive gravity anomalies running along the continental margin and centered over the shelf edge. It is associated with a belt of negative gravity anomalies over the slope and rise throughout the length of the continental margin. This coupled belt of negative and positive gravity anomalies is an edge effect observed along continental margins (Naini and Talwani, 1983).

## Magnetic

Naini and Talwani (1983) have also discussed magnetic observations of the northeast Arabian Sea. Magnetic anomalies to

the west of the Chagos-Laccadive ridge have been identified as sea-floor spreading magnetic anomalies. Magnetic anomalies in the east, however, could not be identified as typical marine magnetic anomalies. Taylor (1968) has prepared a total magnetic contour map and a residual magnetic contour map of the northern Arabian Sea with a contour interval of 100 gammas. According to these maps long-wavelength (greater than 200 km) magnetic anomalies are present over the northwest Indian continental margin and the eastern basin, whereas short-wavelength (less than 200 km) magnetic anomalies are present in the western basin. In general these maps suggest that the northeast Arabian Sea is mostly covered by long-wavelength magnetic anomalies and short-wavelength magnetic anomalies are present to the south and southwest of the Arabian Sea. Le Pichon and Heirtzler (1968) did a magnetic survey of the Indian Ocean and adjacent Arabian Sea but they failed to identify sea-floor magnetic anomalies older than anomaly 5 north of the Carlsberg Ridge. However, Naini and Talwani (1983), using the magnetic time scale of LaBrecque, Kent and Cande (1977) and Heirtzler et al. (1968), identified marine magnetic anomaly 28 (63 Ma) in the western basin (FIG. 3).

## Seismic Refraction and Reflection

Seismic refraction of the northern Arabian Sea was done by Closs, Bungenstock and Hinz (1969) during the International

Indian Ocean Expedition. The seismic sections are for the Karachi embayment and Gulf of Kutch continental margin. These sections show seismic velocity layers beneath the continental slope and rise. These sections extend to a depth of 10 km from sea-level. The section also shows a normal fault beneath the edge of the continental shelf.

Naini and Talwani (1983) have reported refraction velocities from sonobuoy data for the northeastern Arabian Sea. These data show the seismic velocity structure of the eastern and western basins, and the ridges (FIG.4). The following are the findings of Naini and Talwani (1983): In the western basin sediment thickness varies from 1.3 to 4.2 km and the variation in seismic velocity is from 1.7 to 3.8 km/sec. The average crustal thickness of the western basin is about 5 km. The variation of seismic velocity in the crust is from 5 to 7 km/sec. The Moho is at a depth of about 11.5 km and is marked by the layer of seismic velocity 7.9 to 8.3 km/sec. The sediment thickness in the eastern basin varies from 0.3 to 4.3 km and the seismic velocity varies from 1.5 to 4.6 km/sec. The thickness of the crust is about 11 km. The seismic velocity in the crust, below the sediment, varies from 5.4 to 7.2 km/sec. The average depth to the Moho is about 17 km assuming an upper mantle velocity of 8.2 km/sec. The Laxmi ridge has a thin sediment layer of 500 m. The seismic velocity in the sediment varies from 1.7 to 3.9 km/sec. The average thickness of the underlying crust is about 18 km and the variation in seismic velocity is from 5.4 to 7.2 km/sec. Using a velocity of

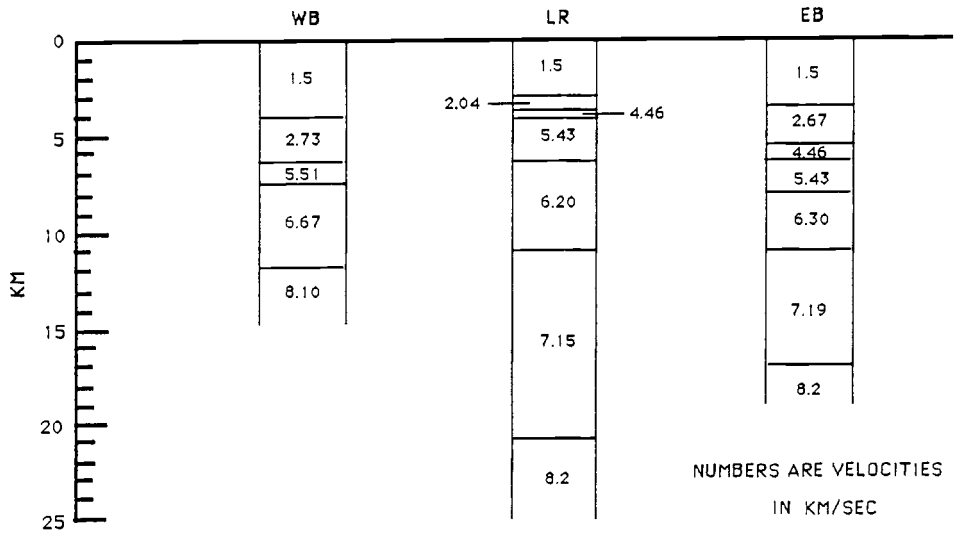


FIG.4 Generalized seismic refraction velocity of the eastern basin (E.B.), the western basin (W.B.) and the Laxmi ridge (L.R.). (Adapted from Naini and Talwani, 1983).

8.2 km/sec the Moho has been interpreted at a depth of about 21 km.

Seismic reflection surveys have also been undertaken by private companies but due to the propriatory nature of the data very little data has been published. Kolla and Coumes (1987) have published some seismic lines which show a sediment thickness of at least 7 km on the shelf off Karachi. The published data failed to reach the basement.

# DATA SOURCES

The geophysical data which are used in this study were requested in digital form from the National Geophysical and Solar-Terrestrial Data Center (NGSDC). The data comprise the residual magnetic and free-air gravity field values at sea-level for the area 14° to 26° N and 60° to 70° E. The data were recorded by different agencies and institutes during the years 1963 to 1981. These agencies were: the University of Tokyo, Scripps Institution of Oceanography, Lamount-Doherty Geological Observatory, the U.S. Naval Oceanographic Office, the Woods Hole Oceanographic Institute and the Institute of Oceanographic Sciences, U.K. The gravity data coverage for the area 14° to 26° N and 60° to 70° E is shown in FIG. 5 and the magnetic data coverage for the region 20° to 26° N and 60° to 70° E is shown in FIG. 6.

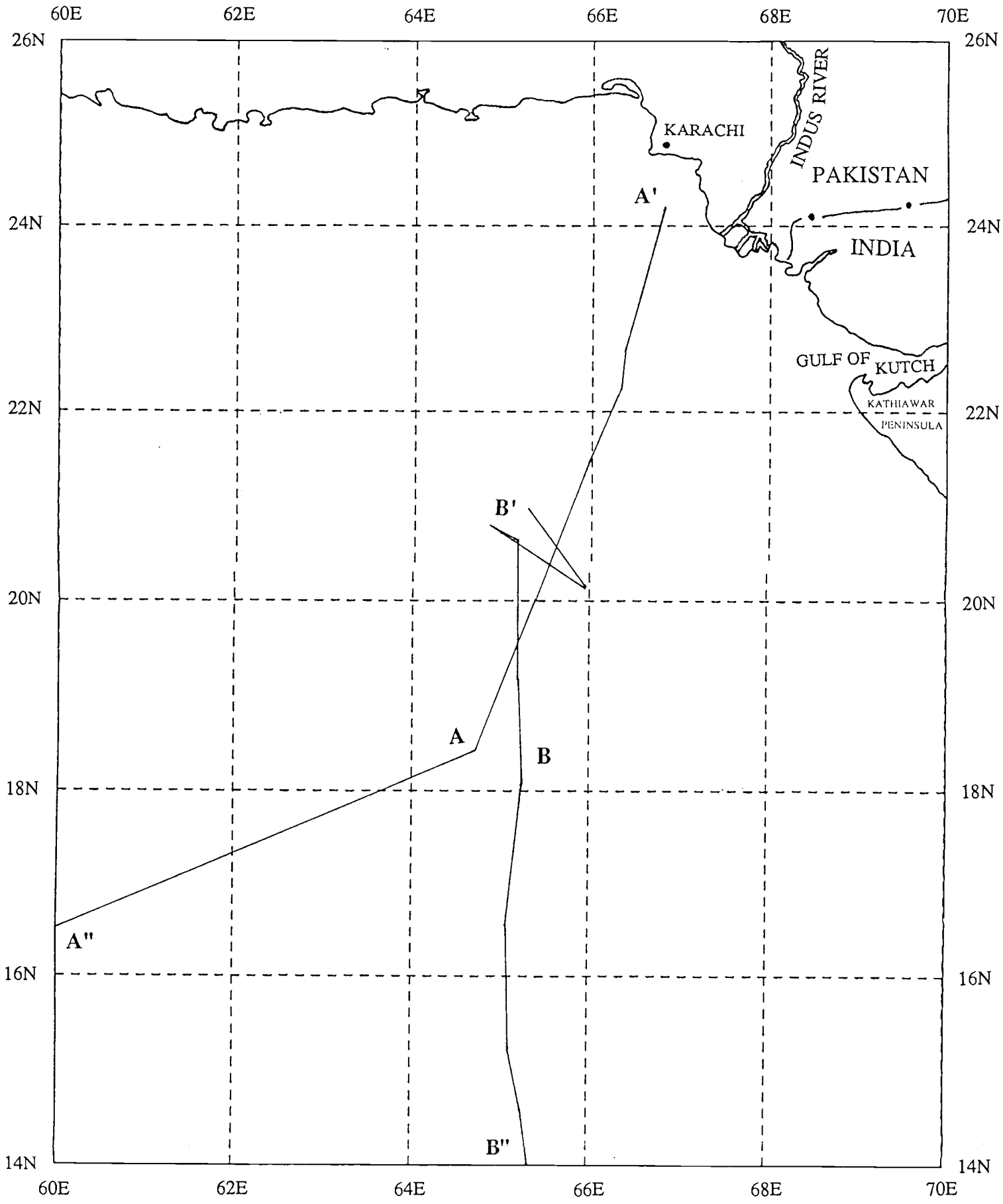


FIG.5 Track line map of the gravity data. Segment AA' of profile A"A' and segment BB" of profile B"B' were combined together to form one profile B"BAA'. The crustal models were developed along this combined profile.

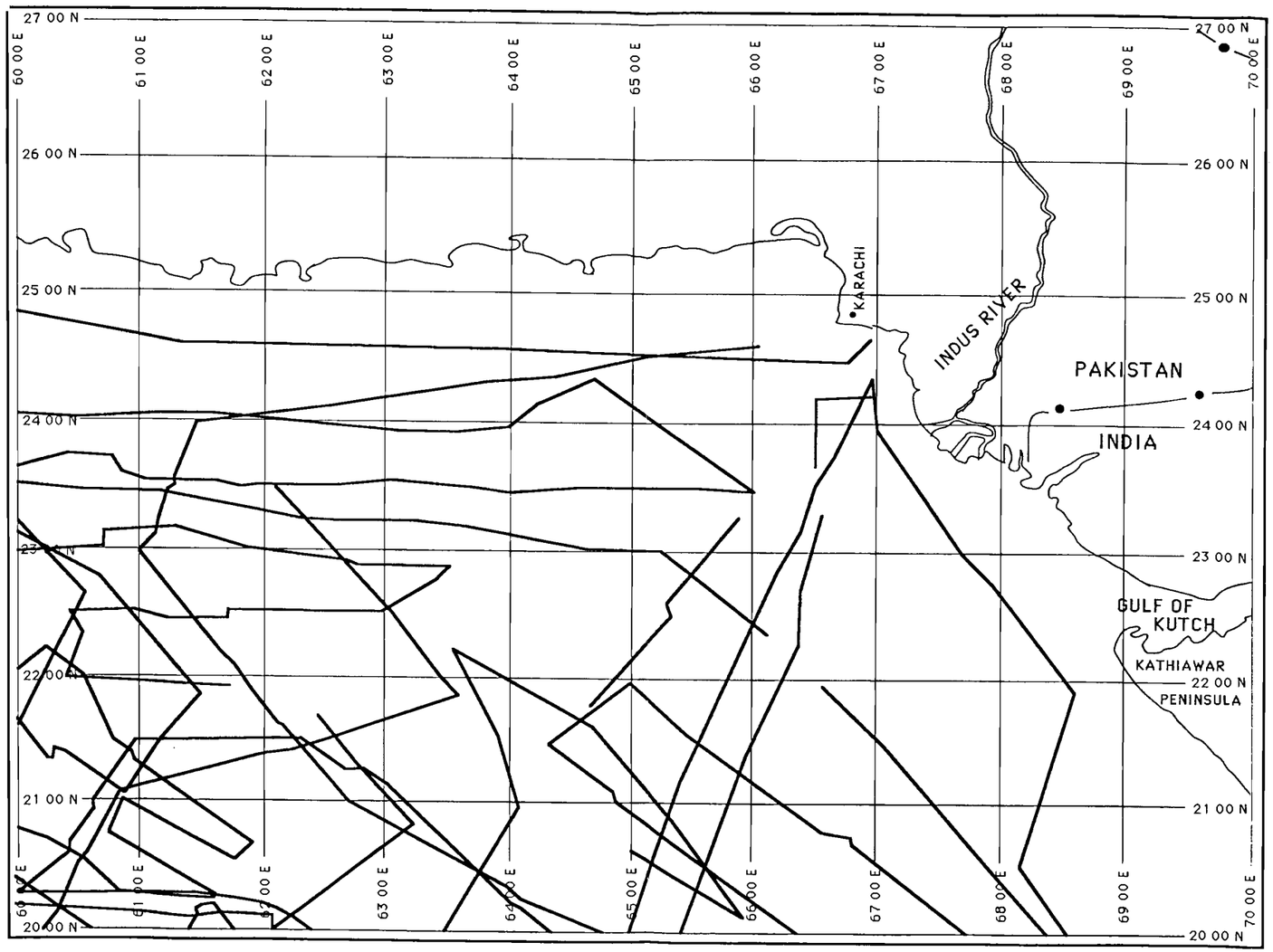


FIG.6 Track line map of the magnetic data used to generate the contour map (FIG.7). The agencies involved are discussed in the text.

# DATA INTERPRETATION

## Magnetic Anomaly Map

A magnetic anomaly map has been prepared using the residual magnetic data obtained after removal of a regional geomagnetic field from the total magnetic field. The processing of the data was done on the PDP11 computer and the computing facilities available at the CONMAR (Continental Margin Research Group). Since the magnetic data were from different sources, they were checked for crossing errors. The initial crossing error was 700 nT which was lowered to 30 nT after two iterations for the correction of crossing errors. The corrected data were then computer contoured using the minimum curvature technique of Briggs (1974). FIG. 6 shows the track lines along which the marine magnetic data were collected.

The magnetic contour map (FIG. 7) covers an area extending from 60° to 70° E and 20° to 27° N. The area covered by the contour map includes the northern region of the Murray ridge, a triangular area of the Makran subduction zone west of the Murray ridge, and the upper Indus fan east of the Murray ridge. The magnetic anomalies in the area vary from 300 nT to -1000 nT.

The region west of the Murray ridge (i.e. the area of the Makran subduction zone) has low-gradient magnetic anomalies. The magnetic anomalies in this region vary from -600 nT to -900 nT and are of long wavelength (greater than 200 km); moving east

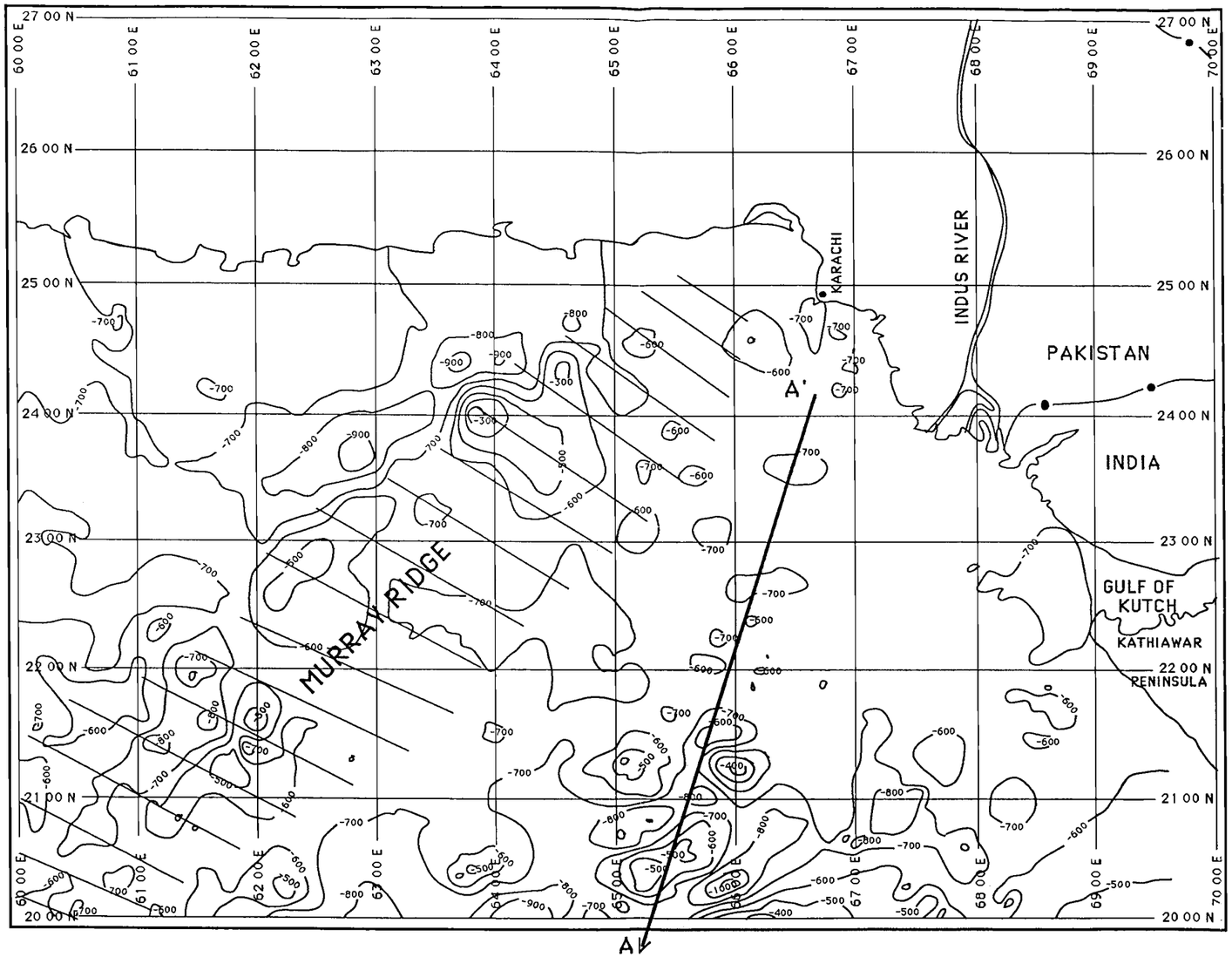


FIG.7 Residual Magnetic Map with a contour interval of 100 nT. Dashed area represents the Murray ridge. A section of profile A-A' is also shown the along which magnetic and gravity models are developed. The map shows short-wavelength anomalies between Murray ridge and west coast of India and long-wavelength anomalies on the other side of the Murray ridge.

to west in this region the magnetic anomalies get shorter in wavelength. There is only one high-gradient, short-wavelength (less than 200 km) magnetic anomaly and from peak-to-peak this magnetic anomaly varies from -600 nT to -800 nT. In this region oceanic crust of the Arabian plate is believed to be subducting beneath the Lut and Afghan blocks (Jacob & Quittmeyer, 1979).

The Murray ridge possesses both low-gradient and high-gradient magnetic anomalies. The bathymetric map of the Murray ridge by Udintsev (1975) shows that it is a topographic ridge. The magnetic anomalies vary from -300nT to -800nT and they generally trend northeast-southwest. The central portion of the Murray ridge in the contour map is covered by long-wavelength, smooth-gradient magnetic anomalies. The northern and southern part of the ridge possesses short-wavelength, high-gradient magnetic anomalies with an average peak-to-peak magnetic anomaly variation of about -400 nT. The distribution of magnetic anomalies over the Murray ridge suggests that in the central portion the magnetic source is deeper than that lying to the north and south.

In terms of the magnetic anomalies the upper Indus fan region (portion of the Indus fan covered by the magnetic map (FIG.7)) can be separated into a northern part and a southern part. The northern part consists of smooth-gradient, long-wavelength magnetic anomalies which vary from -600 nT to -700 nT. There is no clear trend of the magnetic anomalies in this region but there are a few isolated, high-gradient, small-wavelength magnetic anomalies in the upper portion of the area. The small-

wavelength features on the map may be related to basement ridges which might be buried beneath the sedimentary cover or these may be indicative of a magmatic intrusion through a thinned and stretched continental crust.

The southern portion of the upper Indus fan consists of small-wavelength, high-gradient magnetic anomalies. These magnetic anomalies vary from -500 nT to -1000 nT and generally trend in a northeast-southwest direction. A few magnetic anomalies in the eastern part of the area have a north-south trend. Most of the short-wavelength magnetic anomalies are clustered between 60° to 65° E and 20° to 22° N. Looking at the wavelength of the magnetic anomalies and the style of the variation in the magnetic anomalies along the profile it appears that these magnetic anomalies may be indicative of underlying oceanic crust. Naini and Talwani (1983) have also discussed the magnetic anomalies of this region. These authors have failed to find any correlation between these magnetic anomalies from one track line to another track line, which is vital for accepting these anomalies to be from the seafloor. Also according to these authors the anomalies do not match any marine magnetic time scale. The magnetic anomalies to the west of this cluster are very smoothly graded and are almost flat in the area adjacent to the eastern boundary of the Murray ridge.

The map (Fig. 7) shows a cluster of short-wavelength magnetic anomalies along Lat. 20° N. These magnetic anomalies also have been reported by Taylor (1968) who has attributed these to a ridge-like feature buried beneath the great volume of

sediments of the Indus river. In his opinion this buried ridge may be associated with the Murray ridge and Chagos-Laccadive plateau but it is inactive now.

## Assumptions for gravity and magnetic modeling

It has been assumed that no lateral density variation occurs below 50 km depth. The oceanic and continental crusts are approximated by the same density material, which is useful for the interpretation of regional structures and as used by Swift et al. (1987), Hutchinson et al. (1982) and Grow et al. (1979) for studying the U. S. east coast continental margin. For gravity modeling the sediment thickness is approximated by two layers. The depth for the interface between upper and lower sediment layers has been assumed arbitrarily at approximately 3 km depth from the top of the sediment. The lower sedimentary layer gets thinner seaward. Also the crust has been divided into two layers. The interface between the upper and lower crust has been assumed arbitrarily at a depth of about 11 km. The interface is deeper landward than seaward. For gravity modeling a range of densities for each of the layers has been assumed. The assumed range of densities are: 2.0 to 2.2 gm/cc for the top layer of sediment, 2.3 to 2.5 gm/cc for the bottom layer of sediment, 2.6 to 2.8 gm/cc for the top layer of crust and 2.8 to 3.0 gm/cc for the bottom layer of crust. The density of the mantle has been assumed to be 3.4 gm/cc. This value for the density of mantle has

been suggested by Naini and Talwani (1983) on the basis of seismic observations.

In modeling the magnetic anomalies as seafloor anomalies two magnetic layers of the oceanic crust have been assumed with the top thin layer having susceptibility 2 to 3 times higher than the lower layer.

## Constraints for modeling

The modeling of the continental margin off Pakistan has been done around a vertical mass column of 153.71 x $10^2$ kg/cm$^2$ for a 50 km thick section. This mass column corresponds to an attraction of 6442.0 mgal at sea level. This value comes from a compilation by Barday (1974) for a mass of a 50 km thick vertical column. The compilation is based on the sections suggested by Worzel and Shurbet (1955 ), Talwani et al. (1959a), Worzel (1965), and Couch (1969). This compilation shows that the mass of a 50 km thick vertical column of the lithosphere varies from 149.40 x $10^2$ to 154.08 x $10^2$ kg/cm$^2$. In this study a mass value of 153.71 x $10^2$ kg/cm$^2$ is selected as a reference value. In the absence of seismic control the assumption of 6442.0 mgal is very useful and convenient.

Bathymetry was also recorded along with the gravity and magnetic data for profile A-A' and B-B" (FIG 2 & 3) which were used in this study to develop crustal models. Bathymetry was an important constraint in developing the crustal models.

Sonobuoy data along the profile (FIG. 8) were used to constrain the depth of the sediment-crust interface. FIG.9 shows the densities corresponding to the seismic velocities of FIG.8. Following the suggestion of Naini and Talwani (1983) layers with velocity less than 5 km/sec are taken as sediment. Hence the interface across which seismic velocity increases to more than 5 km/sec marks the sediment-crust interface. The depth of this interface varies from about 6 km landward to about 8 km seaward. The Moho depth is constrained only at one point which is located at the seaward end of the profile. This constraint on the depth of Moho comes from the seismic refraction data of Naini and Talwani (1983).

For the magnetic model the top of the magnetic layer is constrained by the sediment-crust interface used for the gravity modeling. To mark the bottom of the magnetic layer an estimation for the depth of Curie-isotherm was done (Appendix) which suggests 18 km as the depth for this thermal boundary between magnetic and non-magnetic layers.

## Gravity model

2-D gravity models were developed for the free-air gravity data along profile A-A' (FIG.5). The gravity data were recorded by the Woods Hole Oceanographic Institute in 1977. The observed relative gravity data were referenced to the IGSN 71 (International Gravity Standardization Net 1971). The free-air

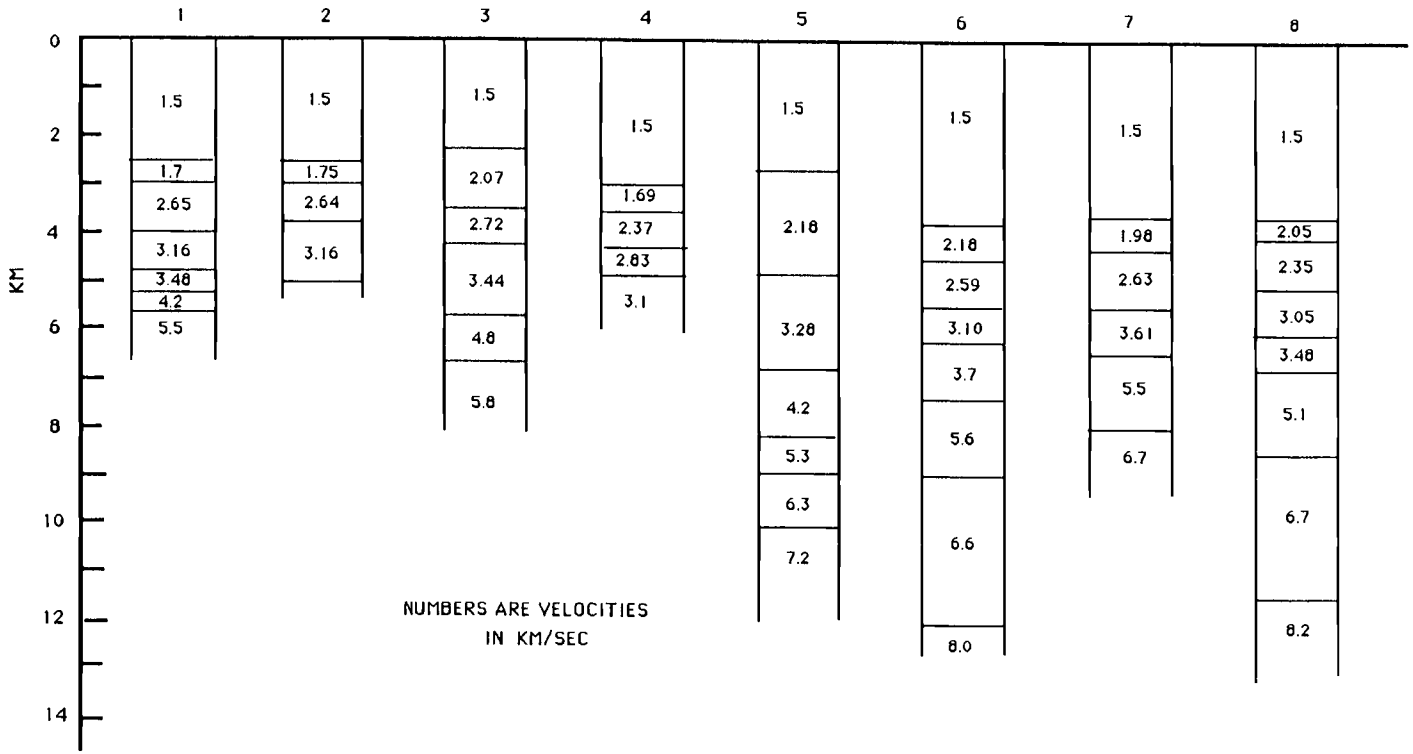


FIG.8 Refraction velocities of crustal sections at different locations along profile A-A' and B-B". The locations are shown in FIG.3. (Modified fram Naini and Talwani, 1983)

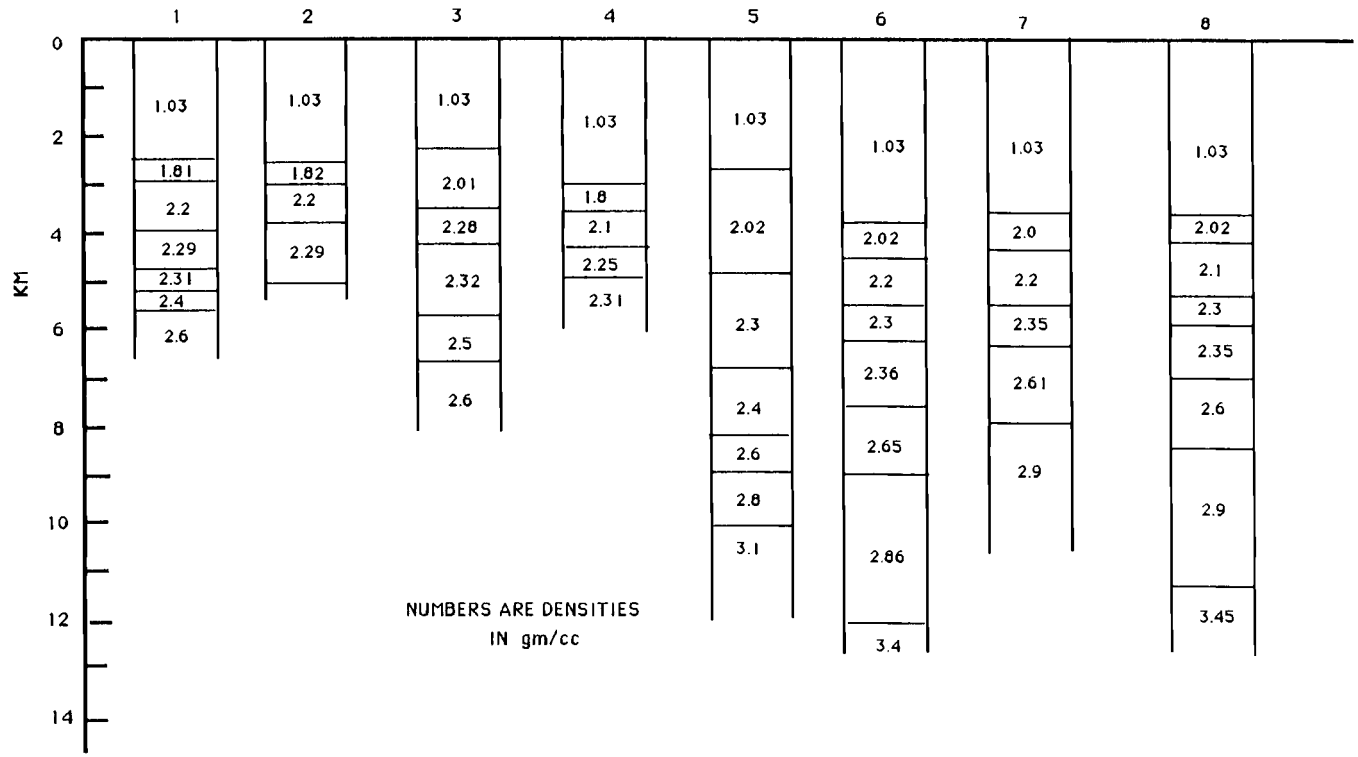


FIG.9 Densities corresponding to the seismic velocities shown in FIG.8. Densities are calculated using the Nafe and Drake curve (Nafe and Drake, 1957).

gravity anomalies were computed using the above obtained gravity values and the Geodetic Reference System 1971. The 2-D gravity modeling was done using a computer program developed at CONMAR (Continental Margin Research Group). The computational algorithm for the 2-D gravity model was based on Talwani et al. (1959b).

The profile selected for modeling starts at 24°13' N, 66°45' E and ends at 18° 24' N, 64° 36' E and is oblique to the western continental margin of India located about 250 km east of the Murray ridge.

For gravity modeling, the upper 50 km of the lithosphere is represented by six layers. These are; a water layer, two sediment layers, two crustal layers and a mantle layer. Bathymetry was the major constraint in developing the model and it marked the water-sediment interface. The bathymetry has a very smooth gradient near the continental margin. At a distance of about 375 km along the profile (Fig. 10) the bathymetry shows a small ridge which seems to be a feature formed by sediment deposition. There was no constraint on the depth of the sediment-crust interface below the continental shelf and upper slope.

Based on seismic constraints the sediment thickness is about 4 km beneath the abyssal plain (FIG. 11). Two refraction stations show sediment thicknesses of about 5 km beneath the lower slope, but the gravity data suggest that the sediments may be up to 9 km thick locally within structures inferred to be rift grabens.

At the seaward end of the profile the Moho depth is constrained by sonobuoy data from Naini and Talwani (1983)

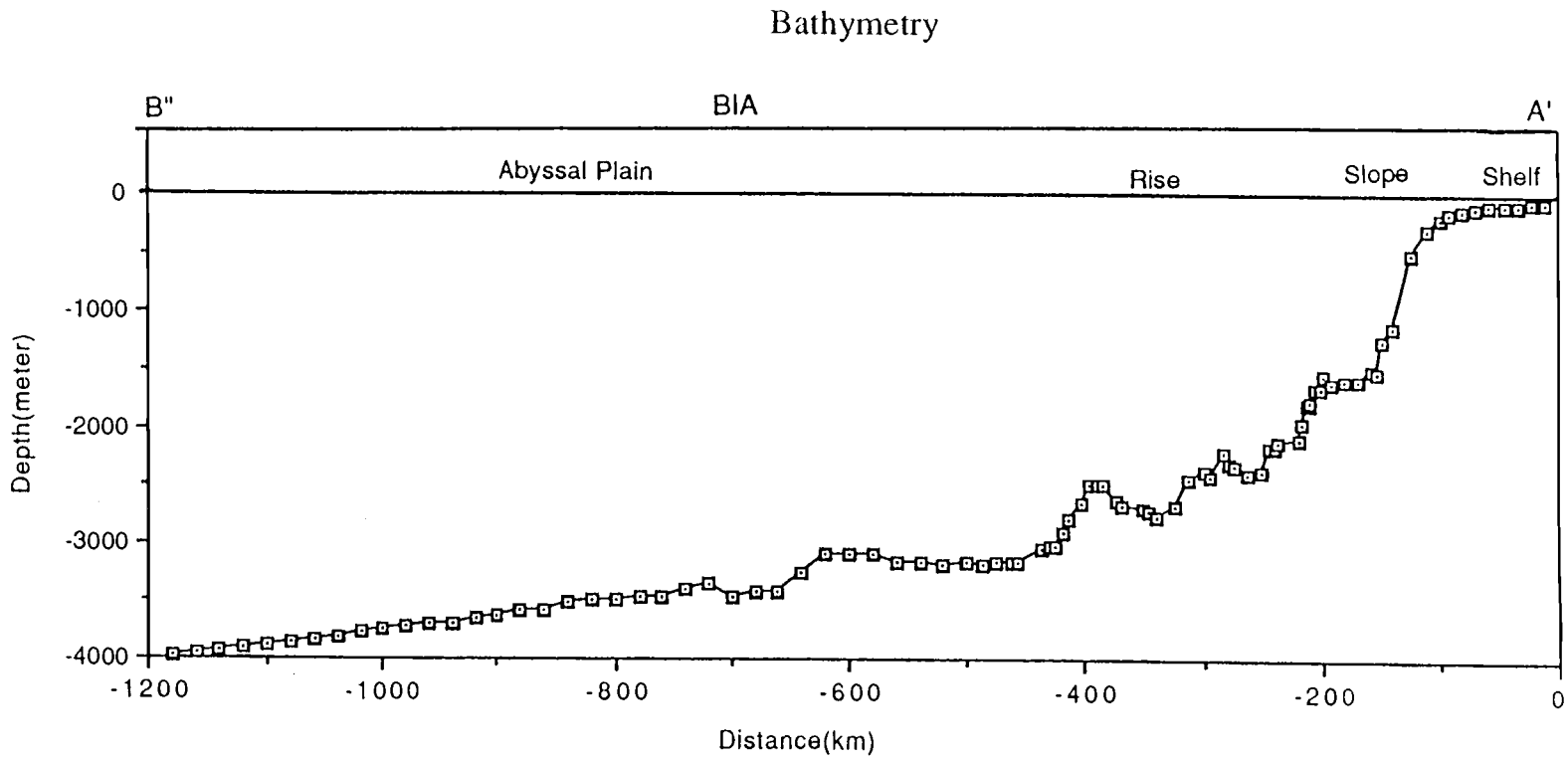


FIG.10 Bathymetry along the profile A-A' and B"-B.

FIG.11 Gravity model along profile A-A'. The depth of Moho shown in the model is one of the many values expected for the depth range of the Moho. The Moho depth at the seaward end is constrained by the seismic data. The gravity models differ from each other with regard to the interpretation of the anomaly at 670 km; (i) in this model the anomaly has been interpreted as due to a fracture zone, fault, or graben, (ii) the second model suggests that the anomaly results from some heterogeneity in the crust, and (iii) the third model shows the continent-ocean boundary as the source of the anomaly. In the figures block (a) is the model, (b) is the observed and calculated anomalies, (c) is the gravity effect of the Moho, the bathymetry and the Moho+bathymetry and (d) is the mass column variation along the model.

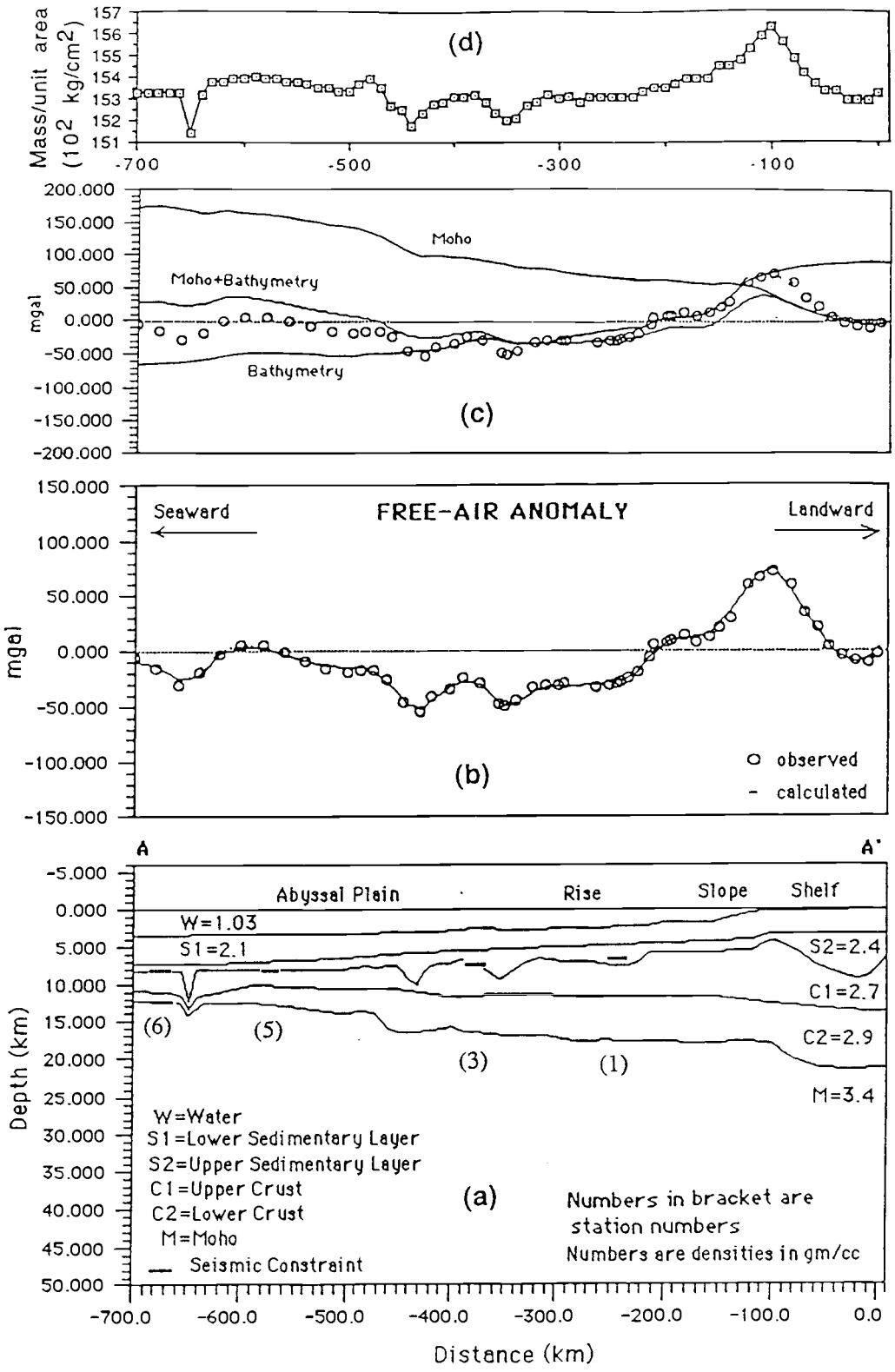
Mass/unit area (10² kg/cm²)
157
156
155
154
153
152
151
(d)
-700
-500
-300
-100
200.000
150.000
100.000
50.000
0.000
-50.000
-100.000
-150.000
-200.000
mgal
Moho
Moho+Bathymetry
Bathymetry
(c)
150.000
100.000
50.000
0.000
-50.000
-100.000
-150.000
mgal
Seaward
FREE-AIR ANOMALY
Landward
(b)
o observed
- calculated
A
A'
-5.000
0.000
5.000
10.000
15.000
20.000
25.000
30.000
35.000
40.000
45.000
50.000
Depth (km)
Abyssal Plain
Rise
Slope
Shelf
W=1.03
S1=2.1
S2=2.4
C1=2.7
C2=2.9
M=3.4
(6)
(5)
(3)
(1)
W=Water
S1=Lower Sedimentary Layer
S2=Upper Sedimentary Layer
C1=Upper Crust
C2=Lower Crust
M=Moho
Seismic Constraint
(a)
Numbers in bracket are station numbers
Numbers are densities in gm/cc
-700.0
-600.0
-500.0
-400.0
-300.0
-200.0
-100.0
0.0
Distance (km)

(i)

FIG. 11

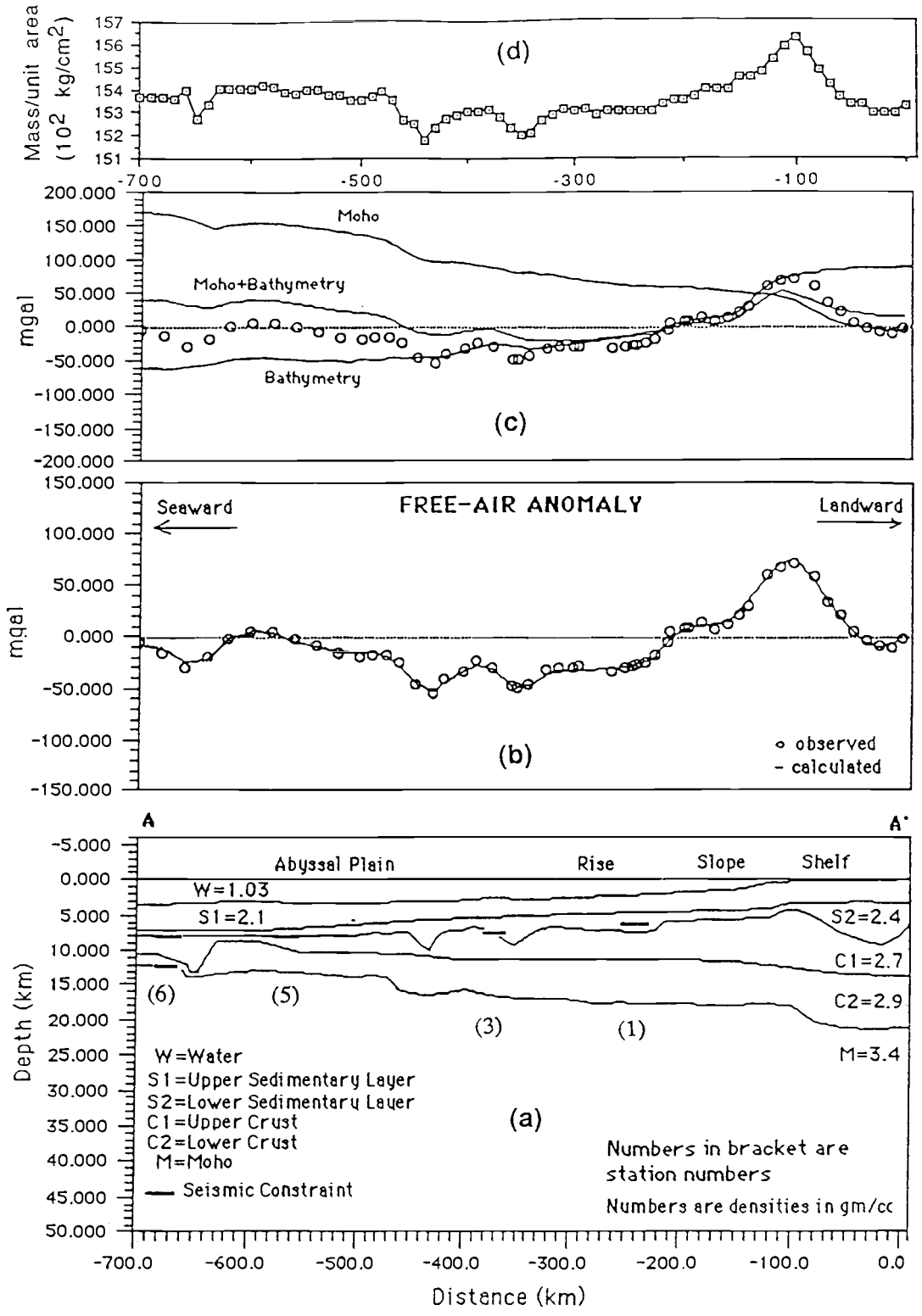


(ii)

FIG. 11 (continued)

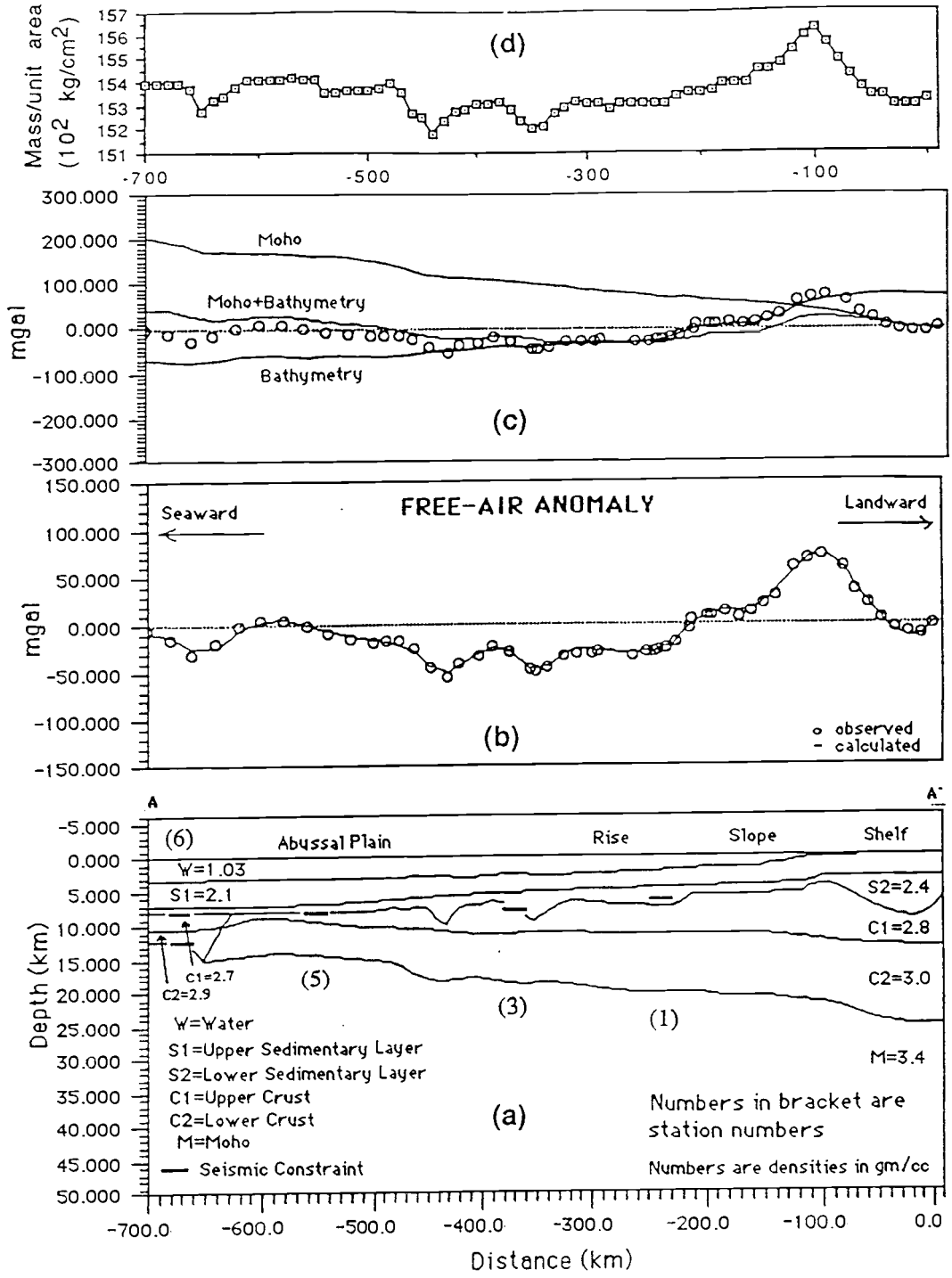


(iii)

FIG. 11 (continued)

(FIG. 11). The Moho depth beneath the shelf, slope and rise is determined solely from the gravity modeling.

Any estimation for the total thickness of the crust or depth of the Moho would be dependent on the density used for the sediment and crustal layers. The seismic stations 1,5 & 6 are on the abyssal plain, stations 2 & 3 are on the lower continental rise and station 4 is on the upper continental rise (FIG. 8 & 9). These data suggest a range of 1.8 to 2.5 gm/cc for the densities of the different layers of sediment. Seismic velocity corresponding to the density of 2.5 gm/cc (i.e. 4.8 km/sec) has been observed at only one location. According to these constraints 2.4 gm/cc is the general density of the lowest sedimentary layer. In the gravity model (FIG. 11, block a) the sedimentary layer has been represented by two layers of densities 2.1 and 2.4 gm/cc. Except at the seaward end of the profile, densities of the crystaline crust are not constrained. Because determination of the depth to the Moho depends on the density of the crust, this approach does not give a unique estimate of the depth but does give a range within which the Moho depth may be expected. The Moho depth shown in FIG. 11 is based on one of the many possible densities of different layers. This model can be used as a reference to discuss the uncertainty in the model.

At about 670 km distance along the profile the observed gravity anomaly shows a negative anomaly of about -30 mgal. FIG. 11 (i-iii) show different interpretations for this anomaly. In FIG. 11 (i, block a) the anomaly has been interpreted as due to a fault or a fracture zone or a graben. Another possibility is shown

in FIG. 11 (ii, block a) where the anomaly has been interpreted as due to some heterogeneities in the crust or due to a graben filled with materials which have the same density as that of the crust. Still another possibility is suggested in FIG. 11 (iii, block a) where the continent-ocean boundary has been interpreted as the source of the anomaly. On the basis of available data it is not possible to determine which of the above possibilities is the most appropriate source for the anomaly.

The mass column variation along the profile is also shown in FIG. 11 (block d). The trend of the mass column variation is similar to that of the observed Free-Air gravity anomaly. The maximum mass column is beneath the continental shelf. The force developed due to variation in the mass of the columns along the profile must have been balanced by the shear strength of the lithosphere modeled in this study.

FIG. 11 (block c) shows the gravity effect for the Moho and bathymetry. The predominant effect on the gravity data is that of bathymetry. The small ridge in the observed gravity data at about 370 km is well correlated with the ridge in the bathymetry at about the same location along the profile. The gravity anomalies above the slope and rise are also in good correlation with the gravity effect of bathymetry for the slope and rise. The gravity effect of the bathymetry, however, results in too large a seaward decrease in gravity which can be counter-acted by a landward thickening of the crust. The combined gravity effect of bathymetry and Moho matches most of the features of the observed gravity anomalies seaward of the slope. This indicates

either: 1) in general homogeneous density layers beneath this region or 2) most of the heterogeneities are such that they cancel each others effect or 3) the Moho is less smooth than shown but balanced by crustal heterogeneities. The models show some of the heterogeneities in the sediment and crust, which were needed to match the calculated gravity with the observed gravity. The mismatch between the observed gravity data and the bathymetry+moho gravity effect above the shelf suggests that either the Moho should be deeper than shown in the model or that there is a basin on the shelf as shown in the model (FIG. 11, block a). The interpretation of basin structure beneath the continental shelf is consistent with the observation of Rehman (1963) and Zuberi & Dubois (1962) (reported in Closs et al., 1969) along with the seismic refraction data for offshore Karachi. Also, the well data reported by Shuaib (1982) indicates basin structure beneath the shelf (FIG. 2).

The gravity model was extended further seaward to a region where crustal thickness was constrained by seismic data, suggesting a typical oceanic crust. For this the profile A-A' was appended with the section B"-B of the profile B"-B' after removing the crossing error between the profile B"-B' and A"-A' (FIG. 5). The average crossing error for three crossing locations was 14.8 mgal. FIG. 12 shows the extended model with one of the possible interpretations discussed in FIG.11 (i-iii).

Because the depth to the Moho shown in FIG. 11 is not a unique solution, an attempt has been made to determine the allowable range for the Moho depth. By assuming the lowest

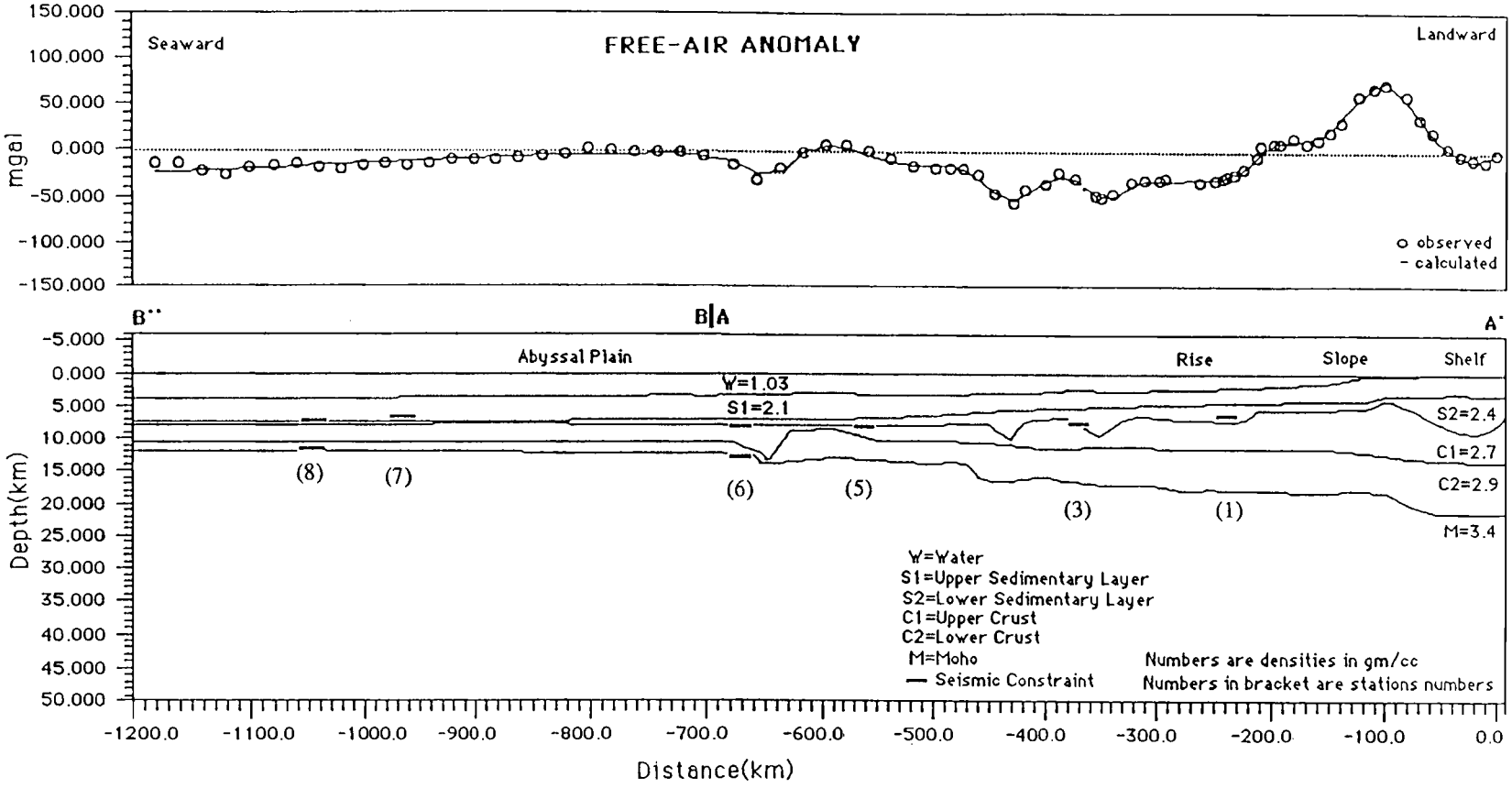


FIG. 12 Gravity model along the profiles B"-B and A-A'. Location shown in FIG. 5. The model shows one of the possible interpretations for the anomaly at 650 km along the profile.

possible densities for the different layers an estimation can be obtained for the shallowest depth of the Moho. Similarly, high densities are assumed for estimating the deepest depth of the Moho. FIG. 13 shows the estimated values for the shallowest and the deepest Moho. Using density values of 2.0 gm/cc for the upper sedimentary layer, 2.3 gm/cc for the lower sedimentary layer, 2.6 gm/cc for the upper crust, 2.8 gm/cc for the lower crust and 3.4 gm/cc for mantle, the depth of Moho is about 10 km at the seaward end and about 17 km at the landward end. Using densities of 2.2 gm/cc for the upper layer of sediment, 2.5 gm/cc for the lower layer of sediment, 2.8 gm/cc for the upper-crust, 3.0 gm/cc for the lower-crust and 3.4 gm/cc for the mantle, the depth of Moho is about 14 km at the seaward end and 26 km at the landward end. At the seaward end an intermediate Moho depth of 12 km is constrained by seismic data.

FIG. 14 show the plot for variations in the depth of the Moho corresponding to the change in density of different layers. The plus and minus values on the scale refers to the increase and the decrease of the Moho depth with respect to a depth of 21.5 km for the landward end and 12 km for the seaward end. FIG. 14 can be used to estimate the depth of the Moho for different values of density. To get an estimation for the depth of the Moho the delta H values are read for each layer corresponding to the selected density. These delta H values are added together and the sum is added to 21.5 km for landward end and to 12 km for seaward end. The figure indicates the sensitivity of the Moho depth with respect to the density of different layers. The estimation suggests

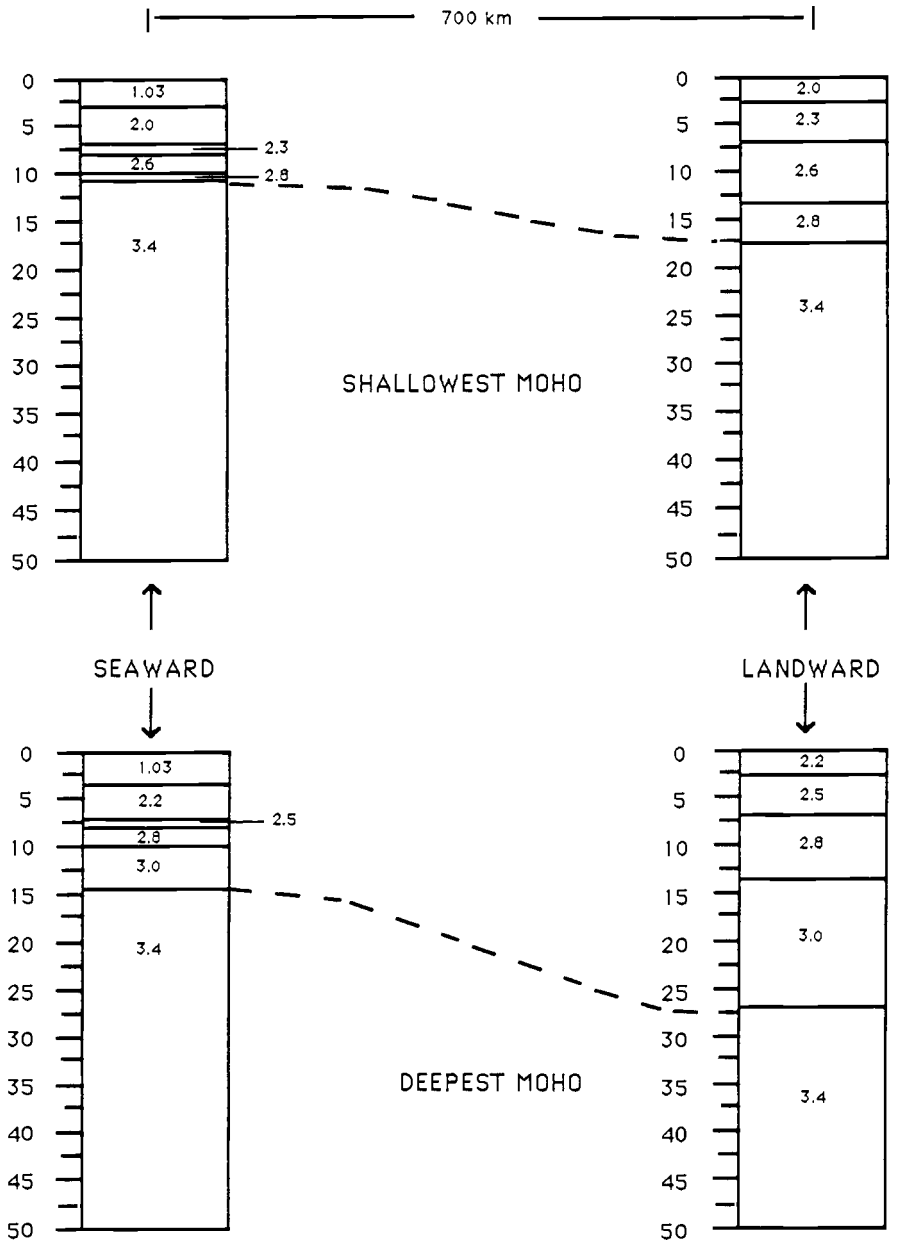


FIG.13 The figure shows the shallowest and deepest depth for the Moho. The Moho depth at the seaward end is however contrained by the seismic data. The above shown variation in the depth of the Moho is calculated using a constant mass column. At the landward end the Moho varies from 17 to 27 km.

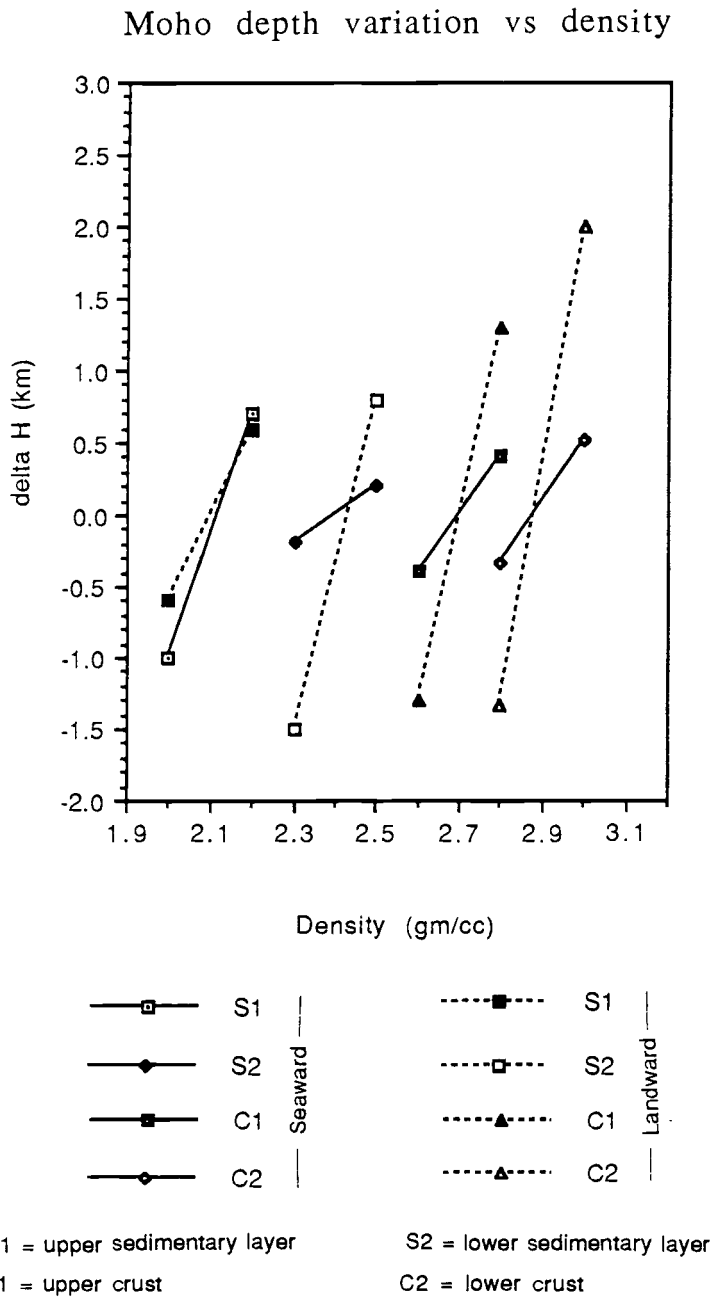


FIG.14 The plot shows the variation in the depth of the Moho corresponding to changes in the density of different layers. For the landward end the delta H values are calculated using 21.5 km as the depth of the Moho. For the seaward end the reference depth of the Moho is 12 km. The plot shows large variations in the depth of the Moho at the landward end.

that depth of the Moho depends on the density of the sediment. As the sediment has the biggest range of the density the depth of the Moho greatly depends on the density of the sediment used. This implies that it is important to have good control on the density of the upper sedimentary layer to minimize the uncertainty. For the landward end, however, the trend is opposite. The Moho depth is more sensitive to the lower crust than the layers above it. Overall, the uncertainty is more at the landward end than at the seaward end.

## Magnetic model

A 2-D magnetic model was also developed for a portion of the profile for which the gravity model was developed. The residual magnetic data along profile A-A' is based on the observed magnetic data and the magnetic reference field IGRF 65 (International Geomagnetic Reference Field 1965). The computational alogrithm for the magnetic model is based on Talwani and Heirtzler (1964). The program was developed at CONMAR. The magnetic modeling requires the inclinations and declinations of the remanent and induced magnetic field. For modeling purposes the declination and inclination of the remanent and induced fields have been kept the same. The declination and inclination values for the region studied in this work are $0^{o}$ and $35^{o}$, respectively (Fig 2.2(a) and Fig 2.2(b) of Merrill and McElhinny (1983)).

The observed magnetic anomalies (FIG. 15) can be interpreted in more than one way. One interpretation could be that the anomalies seaward of the 300 km are seafloor spreading anomalies and the anomalies landward of the 300 km mark are from grabens and rift basins on the crust of continental origin. Another possible source for all these anomalies could be grabens filled with basalts and the volume of magnetic material is greater seaward of 300 km than landward of it. Still another possibility is that a large volume of intrusive dikes are present seaward of 300 km and some shallow magnetic bodies lie beneath the continental slope and rise. The observed anomalies can also be a combination of the above mentioned possibilities.

FIG. 15 shows the model assuming that the anomalies seaward of 300 km are oceanic sea-floor spreading anomalies. For magnetic modeling the magnetic layer (i.e. Curie-isotherm to the sediment-crust interface) is divided into three layers. The Curie depth used is 18 km which is based on the computational technique of Spector and Grant (1970) and is explained in the appendix. The susceptibility of the top layer of oceanic crust is 2-3 times greater than that of the lower oceanic layer (Fox and Opdyke, 1973), the assumed susceptibilities are 0.0015 for the top layer and 0.0005 emu/cc for the bottom layer. For the magnetic layer bounded by the Moho and the Curie-isotherm the assumed susceptibility value is 0.0001 emu/cc. The theoretical anomalies from the seven blocks of alternate magnetic polarity (FIG. 15) approximately matches the observed magnetic anomalies. However, there is considerable mismatch between the observed

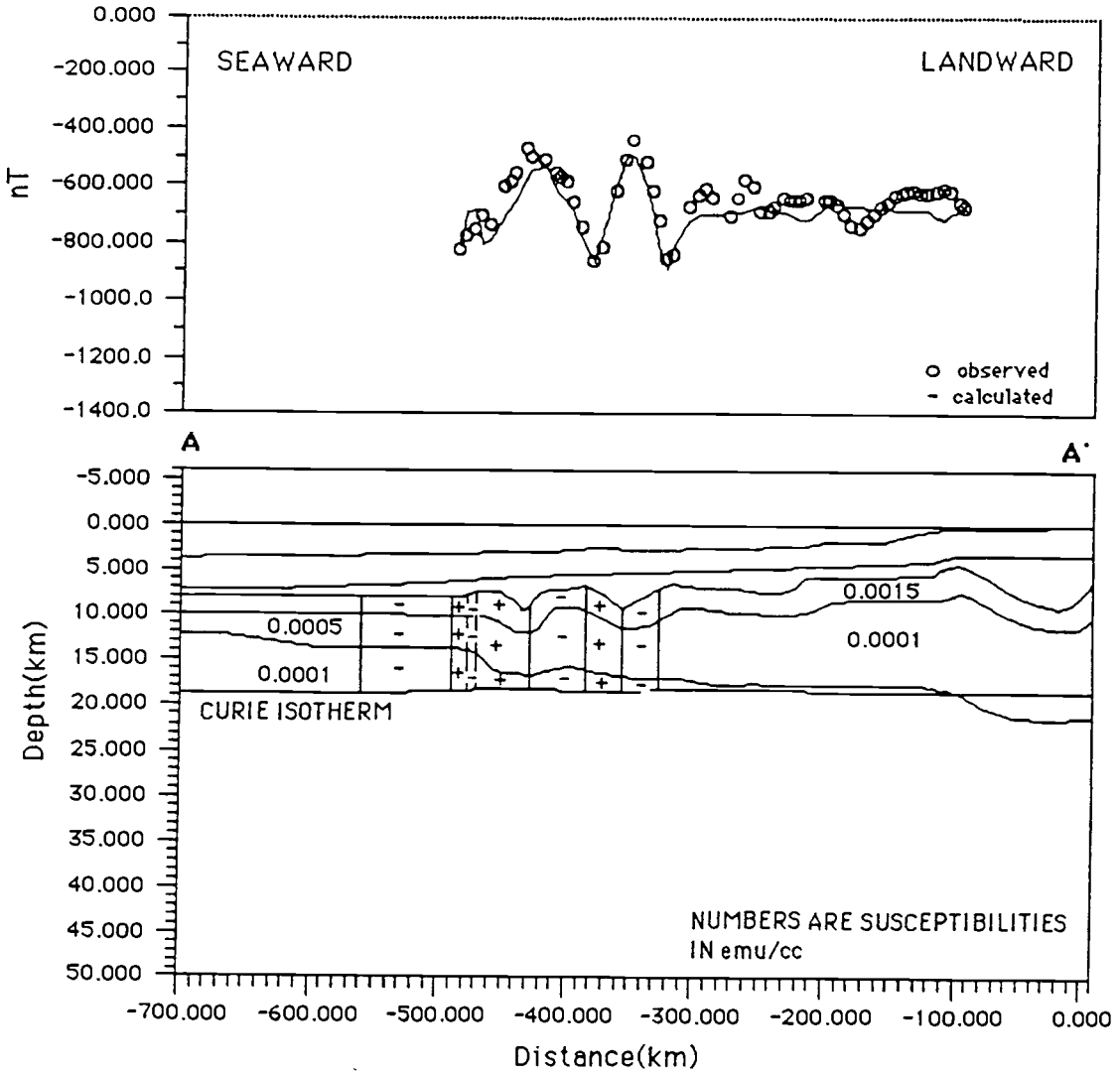


FIG.15 Magnetic model along profile A-A'. Oceanic crust has been assumed as source for the observed magnetic anomalies. The model gives good correlation between the observed and calculated anomalies seaward of the 300 km mark. However, landward of the 300 km mark there is no matching between the observed and calculated anomalies.

and calculated anomalies for the region landward of the 300 km mark. These anomalies may not be from the oceanic crust.

To check whether the oceanic blocks as shown in FIG. 15 are consistent with a magnetic time scale, their location relative to marine magnetic anomaly 28 is compared with the marine magnetic time scale of Harland et al. (1982). FIG. 16 shows this comparison. The observed magnetic data shown in FIG. 15 was appended with more observed magnetic values to extend the profile to marine magnetic anomaly 28. A computer program was then used to compare the observed anomalies with the theoretical marine magnetic anomalies. The inclination, declination and azimuth of the profile were input to the program. Several spreading rates were tried. FIG. 16 shows the correlation between the observed and calculated anomalies for a spreading rate of 40 mm/yr. Between the 600 and 400 km distance along the profile there is some correlation between the peaks of the observed and calculated anomalies. However, seaward of 600 km distance and landward of 300 km distance there is no match between the observed and calculated anomalies. A better comparison however, can be obtained by rotating the observed anomalies to the magnetic north pole. On the basis of the analysis shown in FIG. 16 it is difficult to decide whether the observed anomalies are from oceanic crust or not. Another observation which should be considered in deciding the source of these anomalies is the lineation of these anomalies shown in FIG. 7 (magnetic anomalies north of latitude $20^{o}$ N). These anomalies have lineations perpendicular to the continental margin instead of

FIG.16 The figure shows comparison of the observed magnetic anomalies with the theoretical magnetic anomalies calculated using the magnetic time scale of Harland, et.al. (1982). The analysis was done using a computer program. The standard (theoretical) magnetic time scale was generated using a spreading rate of 40 mm/yr. The calculated and observed anomalies show some matching of the peaks between 600 and 300 km distance. There is no correlation between the observed and calculated anomalies seaward of 600 km and landward of 300 km distances.

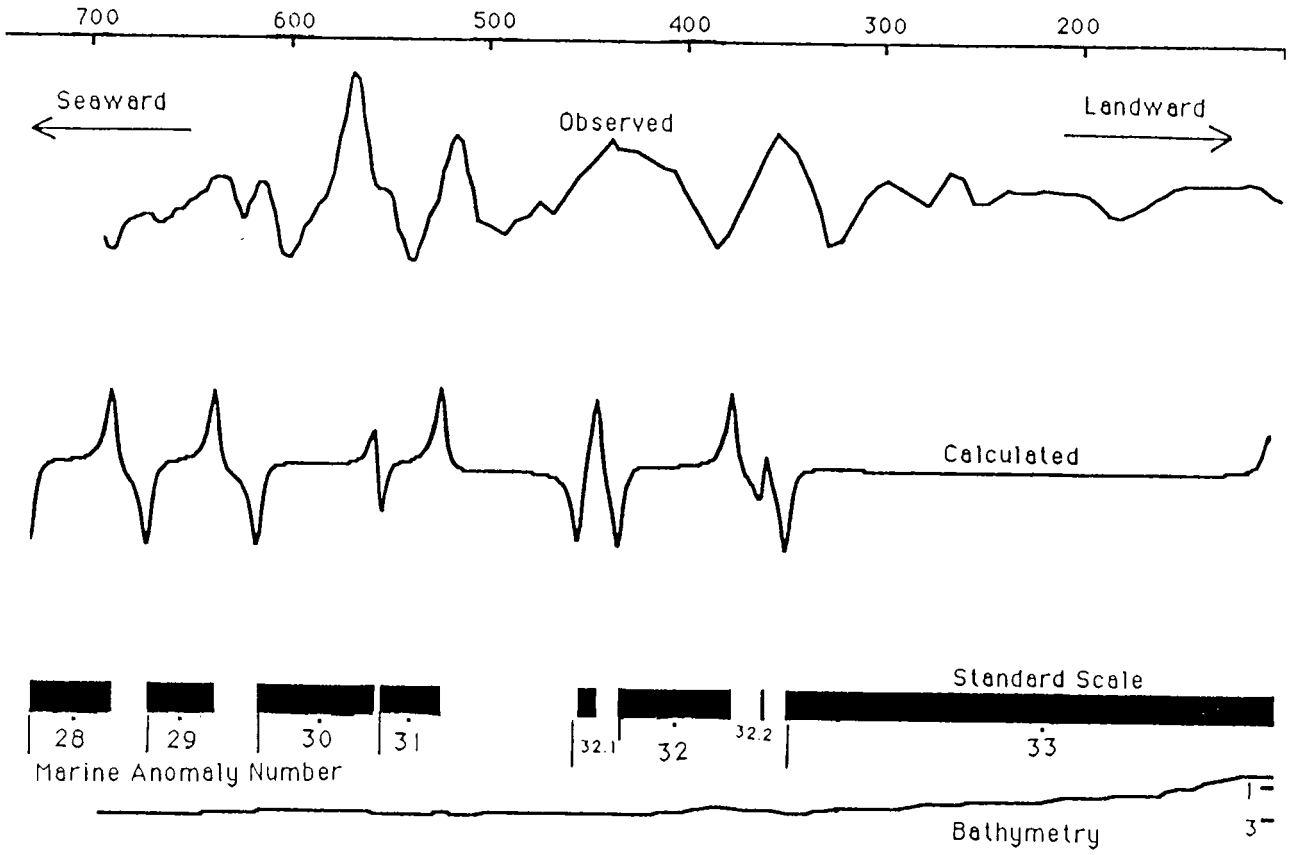
700
600
500
400
300
200
Seaward
Observed
Landward
Calculated
Standard Scale
28
29
30
31
32.1
32
32.2
33
Marine Anomaly Number
1
3
Bathymetry

FIG.16

being parallel to the margin, which is expected for a rifted continental margin. The inland geology north of the study area suggests a rifted continental margin in the study area.

2-D magnetic models assuming other possible sources for the magnetic anomalies can also be developed to match the observed anomalies. A good constraint on the crustal thickness and density would be helpful in distinguishing between oceanic and continental crust. FIG. 17 shows one of the possible alternate models for the observed magnetic anomalies. In this model extrusive rocks have been assumed to be lying at the sediment-crust interface.

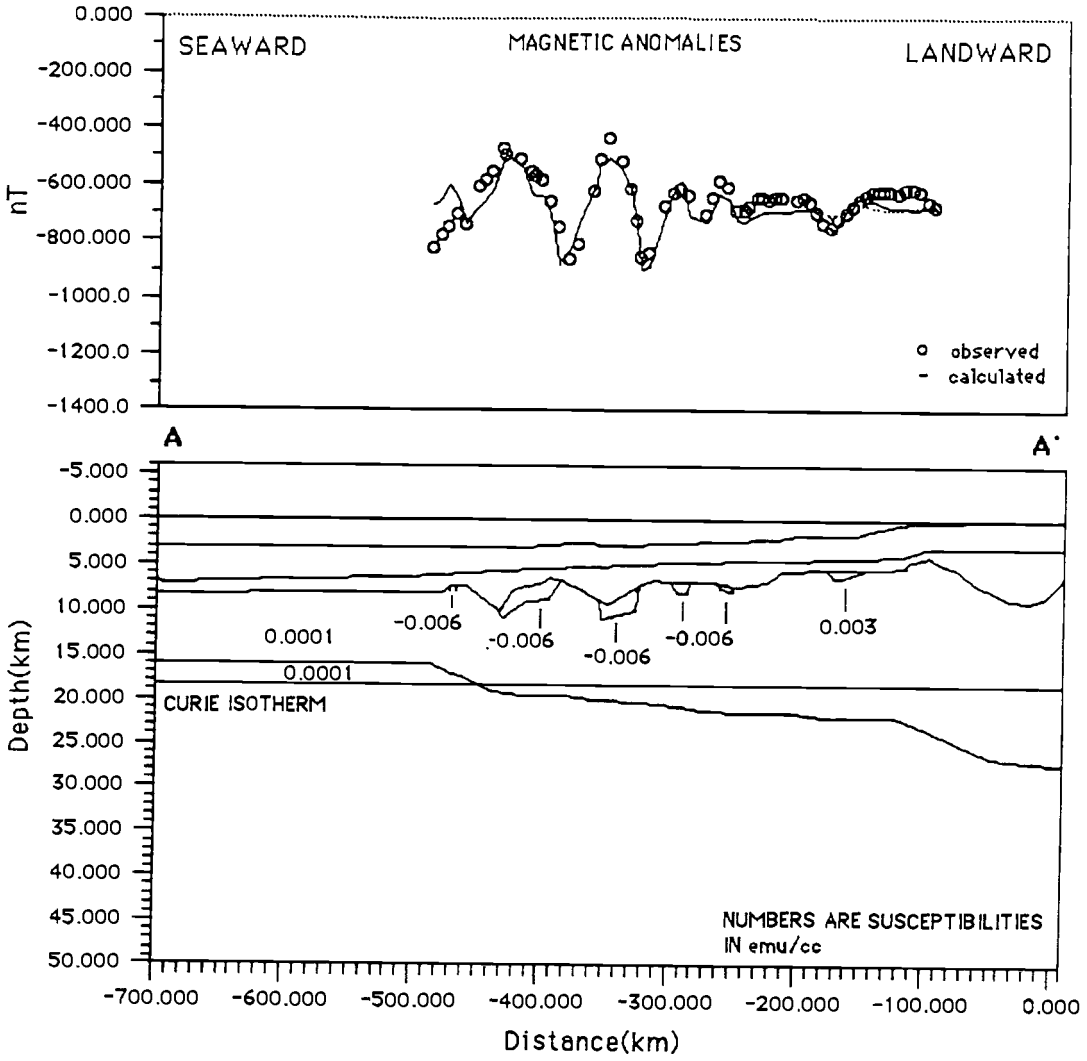


FIG.17 The figure shows an alternate model for the observed magnetic anomalies. Extrusive rocks at the surface of the basement have been assumed as magnetic sources. The model shows good correlation between the observed and calculated anomalies.

# DISCUSSION

The gravity and magnetic models of the continental margin of southern Pakistan can be interpreted as a seaward extension of the rift zone of western India. Several geophysical studies have been undertaken in the region south of my study. Bhattacharya and Subrahmanyam (1986) showed the presence of horst-and-graben structures in the west Indian continental margin off Kathiawar on the basis of magnetic data. In the inland Kutch and Kathiawar region, Biswas (1982), showed rift basins and horst-and-graben structures (FIG. 3).

Kazmi (1979) and Quittmeyer et al. (1979) have reported a 16 June, 1819 earthquake of east-west strike in the Rann of Kutch (FIG. 2 & 3 ). The movement along the fault was dip-slip, down-to-the-south. This normal-faulting type of motion is consistent with the thermal cooling of this continental margin and supports the extrapolation of this study that a transitional crust is present in the Rann of Kutch.

This study suggests that transitional rifted crust extends far offshore beneath the continental margin. The comparison of the continental margin interpreted in this study with the characteristics of the rifted and sheared margins discussed by Scrutton (1982) suggests that the margin off Karachi is a rifted margin. The wide rift zone, as interpreted for the continental margin off Karachi, may be indicative of a long evolutionary history for this margin as suggested by Mutter et al., (1988) for

the Norwegian-Rockall Bank and its conjugate eastern Greenland continental margin and the continental margins off western Australia and Antarctica.

At the seaward end of profile A-A' the gravity data show a significant anomaly of about -30 mgal. FIG. 11 shows fault, fracture zone, graben, internal heterogeneities in the crust and the edge effect of continent-ocean boundary as the probable source for the anomaly. Seismic constraint beneath the anomaly suggests oceanic crust in that area. If the oceanic crust extends landward of this anomaly then it would be more appropriate to interpret this anomaly as a fracture zone or some heterogeneity in the oceanic crust. However, if continental crust is present landward of this anomaly then it could be either a graben or fault. An edge effect of continent-ocean boundary could also be another possibility.

Klootwijk (1979) has suggested counterclockwise rotation of the Indian plate during Mesozoic time. It is possible that the observed anomaly at about 670 km along the profile is due to a fracture zone which was an active transform fault during Mesozoic time.

The modeling of gravity data incorporating the limited available seismic constraints does not give a unique solution for the depth of Moho. However, the analysis gives a wide range of variation (17 to 26 km) for the depth of the Moho. This range is widest at the landward end of the model. At the seaward end, the Moho depth is constrained by seismic data. To suggest a reasonable depth for the Moho, the region around the study area

may be taken as an example. Naini and Talwani (1983), on the basis of seismic study and gravity measurements, have suggested 17 km to be the depth of the Moho in the eastern basin. Also, near Bombay, Kaila et al. (1979) have mentioned 25 to 20 km as the depth of the Moho (as cited by Biswas, 1982). These values fall within the range estimated (17 to 26 km) for the depth of the Moho at the landward end of the profile.

The magnetic study in this thesis failed to confirm the presence of oceanic crust north of magnetic anomaly 28 in the western Indian Ocean. However, a source of evidence to determine whether oceanic crust may be expected north of marine magnetic anomaly 28, is the plate reconstruction for the Mesozoic time period when breakup of Gondwanaland occured. The plate reconstruction by Barron et al., (1978) and other reconstructions reviewed by the above authors (FIG. 18) does not show a good fit of the offshore region of Karachi with Africa. However, a plate reconstruction for Phanerozoic time by Gahagan and Ross (1987) shows that at 180 m.y.B.P the offshore region south of Karachi abutted Africa. According to Gahagan and Ross (1987), India separated from Africa around 166 m.y.B.P (FIG. 19). Considering this plate reconstruction, oceanic crust may be expected in the offshore region south of Karachi. Following the magnetic time scale of Harland et al. (1982) the expected marine magnetic anomaly would be of M29 and younger. However, this study does not confirm that.

A comparison of the gravity profile used in this work with that used by Swift et al. (1987), Hutchinson et al. (1982) and

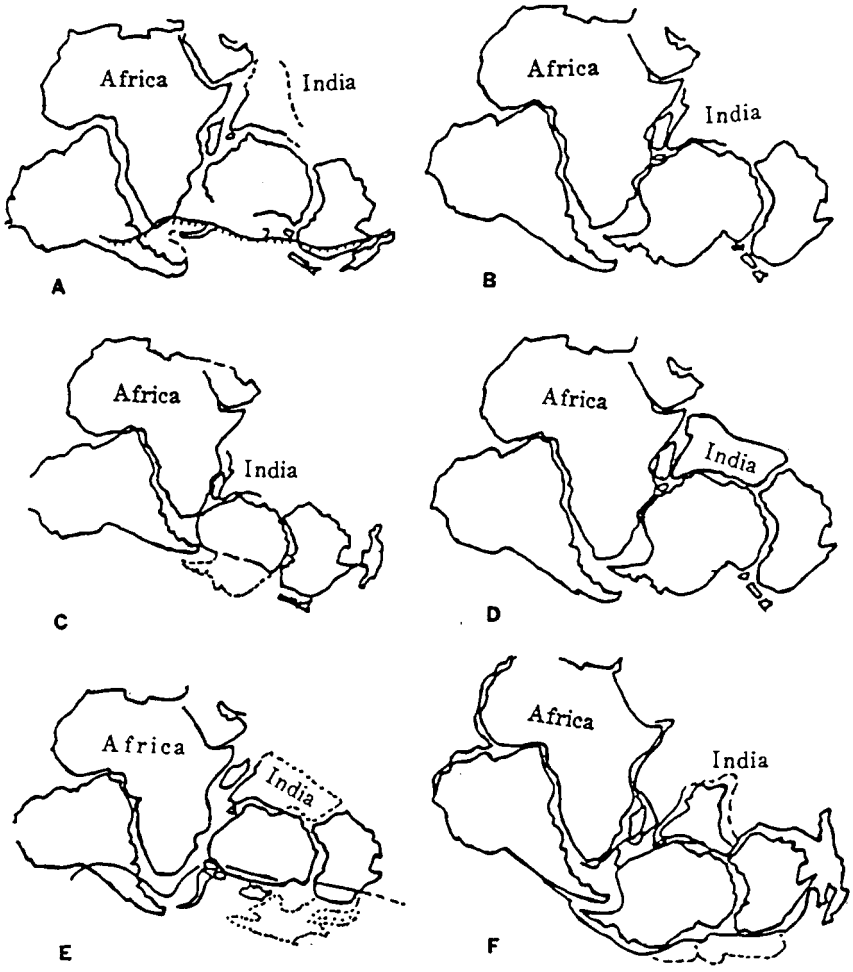


FIG. 18 The figure shows some of the reconstruction for India, Africa and other southern continents. (A) du Toit (1973), (B) Smith and Hallam (1970), (C) Tarling (1972), (D) Veevers et al., (1975) (E) de Wit (1977) and (F) Barron et al., (1977). The reconstructions show controversy in the fitting of India with Africa. (Modified from Barron et al., 1978).

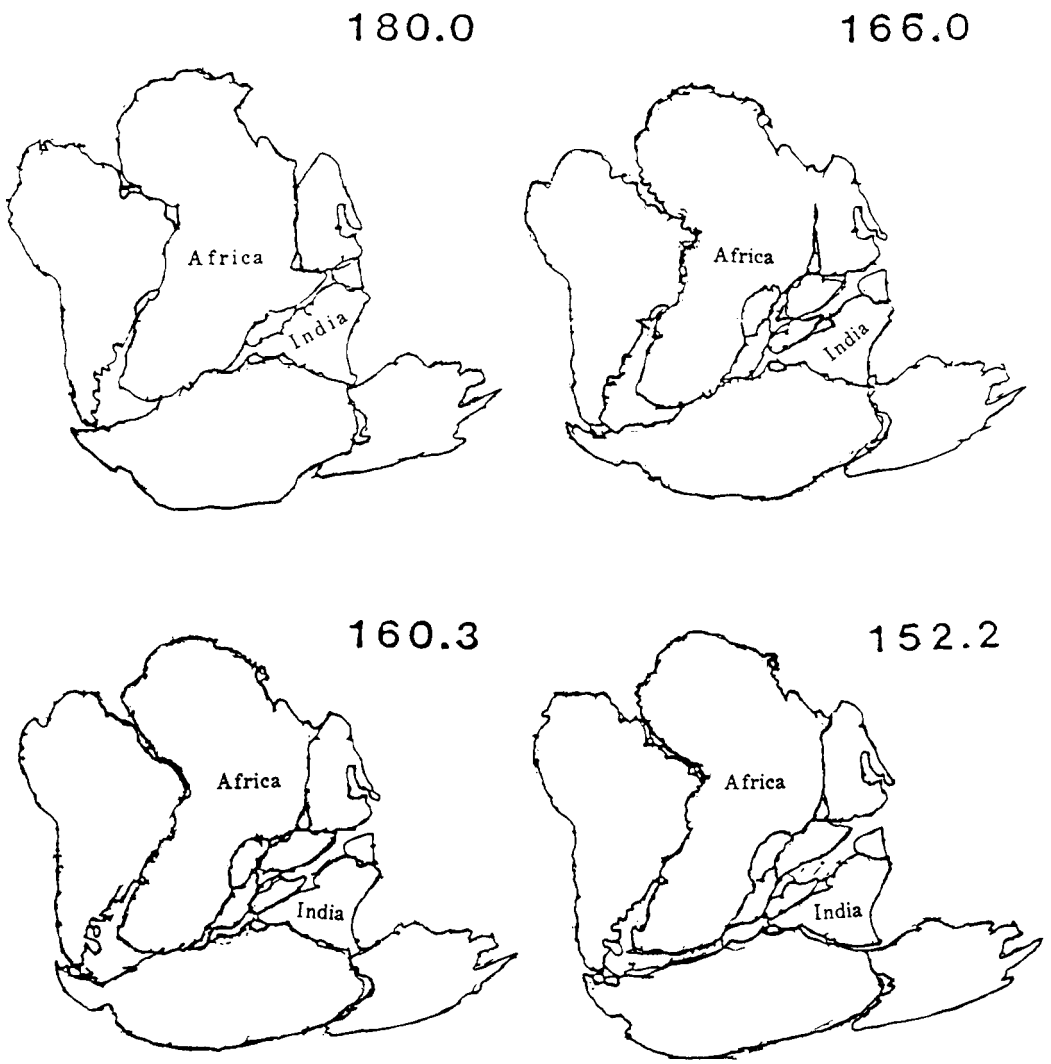


FIG. 19 The figure shows the position of India with respect to Africa during Jurassic time. Between 180.00 to 152.00 m.y.B.P India moved away from Africa. This separation may have formed marine magnetic anomalies of age M29 and younger. (Modified from Gahagan and Ross, 1987)

Grow et al. (1979) to study the United States Atlantic coast suggests that the "edge effect" observed along the gravity profile off Pakistan does not have a sharp negative trough. The profile, however, shows the positive peak landward of the continental margin. This peak may be a part of the edge effect anomaly generally observed on the continental margin. The obscured negative trough of the "edge effect" may be partially due to the low dip of the moho in the transition region between the continental crust and the oceanic crust and it may also be due in part to sediments deposited on the continental slope and rise. These factors will also lower the positive peak associated with the edge effect. The positive and negative peaks of an edge effect are linked together therefore having a positive peak on the shelf without a negative peak seaward indicates the presence of a high density mass beneath the outer continental shelf.

The interpretation of the crustal model for the continental margin off Karachi is analogous to the continental margin observed off southern Australia and its conjugate Antarctic continental margin by Willcox and Stagg (1990), Moore and Eittreim (1987) and Eittreim et al. (1985) in the Bay of Biscay by Le Pichon and Barbier (1987) and in eastern Canada by Keen (1982). They all have a wide stretched zone with extensive thinning of the continental crust from 30 to 15 km. However, the stretched zone is wider (more than 500 km) off Karachi than in the examples mentioned above (350-100).

The calculation (appendix) suggests 18 $\pm$ 1.6 km, as the depth of the bottom surface of the magnetic layer of the

lithosphere. This surface can be either a thermal boundary or a lithological boundary between magnetic and non-magnetic layers of the lithosphere (Shuey et al., 1977; Connard et al., 1983). A lithological boundary forms due to vertical changes in the crustal composition from a magnetic to a non-magnetic composition (Shuey et al., 1977; Connard et al., 1983). The thermal boundary forms at a depth where the temperature increases downward beyond the temperature at which rock loses its magnetic property (i.e. the Curie-point). A lithologic unit may continue downward beyond this interface (Bhattacharyya, 1966; Bhattacharyya and Leu, 1975; Shuey et al., 1977; Connard et al., 1983). The thermal boundary can be associated with the Curie-point of magnetite (Bhattacharyya and Leu, 1975; Shuey, et. al., 1977) which is approximately 580° C (Bhattacharyya and Morley, 1965). If the depth of 18 $\pm$ 1.6 km, as calculated in the appendix, represents a thermal boundary beneath the continental margin off Pakistan then it can be assumed that it represents the 580° C isotherm. A geothermal gradient can then be calculated for the continental margin off Pakistan by assuming 0° C as the temperature of the water bottom. This assumption gives an average thermal gradient of 32° C/km beneath the continental shelf and slope. This value is greater than the average thermal gradient of 30° C/km for the earth (Garland, 1979, p. 346) and if this is correct high heat flow is expected in the offshore region of Karachi.

The area of this study is the offshore region adjacent to the Chaman Fault where the Indian plate is underthrusting the Eurasian plate (Humayun, 1991; Lillie, 1991). The

continent/ocean transition zone modeled in this study is the closest undisturbed zone and may serve as a "templet" for the paleo-passive continental margin that is progressively underthrusting the Eurasian plate along the western edge of the Indian plate.

# CONCLUSIONS

This study suggests that the continental margin off Karachi is a rifted margin with a wide transitional zone and extensive thinning of the crust. The major conclusions of this study are:

a) beneath the continental shelf the depth of the Moho should not be deeper than 27 km and shallower than 17 km.

b) the crust thins gradually from land to sea in a zone about 700 km wide. The characteristics of the crust in this zone may be oceanic or continental. The data used in this study is insufficient to decide on the characteristics of the crust.

c) graben structures may be present at 450 and 350 km distance along the profile which may have formed due to stretching of the continental crust at the time of rifting. At 650 km distance there may be a fracture zone, fault, graben or continent-ocean boundary.

d) this study failed to identify the continent-ocean boundary for the continental margin off Karachi but suggests that it should be located at a distance of at least 500 km and possibly as much as 650 km along the profile.

e) the curie depth which assumes a temperature of 580° C lies at a depth of about 18 km.

# REFERENCES

Admiralty, 1963, Bathymetric, magnetic and gravity investigations, H.M.S 'Owen' 1961-1962, Admiralty Mar. Sc. Publ., no.4, parts 1 and 2, Admiralty Hydrographic Dept., Publ. H. D. 539, 58 pp. and 36 pp.

Barday, R. J., 1974, Structure of the Panama Basin from marine gravity data, M.S.Thesis, Oregon State University, 99 p.

Barron, E. J., Harrison, C. G. A. and Hay, W. W., 1978, A revised reconstruction of the Southern Continents, Eos, Transaction, American Geophysical Union, vol. 59, p. 436-449.

Bhattacharyya, B. K., 1966, A method for computing the total magnetization vector and the dimensions of a rectangular block-shapped body from magnetic anomalies, Geophysics, vol. 31, no. 1, p. 74-96.

Bhattacharyya, B. K. and Leu, L., 1975, Analysis of magnetic anomalies over Yellowstone National Park: Mapping of Curie point isothermal surface for geothermal reconnaissance, Journal of Geophysical Research, vol. 80, no. 32, p. 4461-4465.

Bhattacharyya, B. K. and Morley, L. W., 1965, The delineation of deep crustal magnetic bodies from total field aeromagnetic anomalies, Journal of Geomagnetism and Geoelectricity, vol. 17, no. 3-4, p. 237-252.

Bhattacharya, G. C. and Subrahmanyam, V., 1986, Extension of the Narmada-Son lineament on the continental margin off Saurashtra, western India as obtained from magnetic measurements, Marine Geological Researches, vol. 8, p. 329-344.

Biswas, S. K., 1982, Rift basins in western margin of India and their hydrocarbon prospects with special reference to the Kutch Basin, American Association of Petroleum Geologists Bulletin, vol. 66, no. 10, p. 1497-1513.

Briggs, I. C., 1974, Machine contouring using minimum curvature, Geophysics, no. 1, vol. 39, p. 39-48.

Chowdary, L. R., 1975, Reversal of basement block motions in Cambay basin, India and its importance in Petroleum exploration, American Association of Petroleum Geologists Bulletin, vol. 59, p. 84-96.

Closs, H., Bungenstock, H. and Hinz, K., 1969, Results of seismic refraction measurements in the northern Arabian Sea, a contribution to the International Indian Ocean Expedition, in: Meteor Research Results, no. 2, Sr. C, p. 1-28.

Connard, G., Couch, R. and Gemperle, M., 1983, Analysis of aeromagnetic measurements from the Cascade Range in Central Oregon, Geophysics, vol. 48, no. 3, p. 376-390.

Couch, R. W., 1969, Gravity and structures of the crust and subcrust in the northeast Pacific ocean west of Washington and British Columbia, Ph.D Thesis, Corvallis, Oregon State University, 179 p.

Duroy, Y., et. al., 1989, Subsurface densities and lithospheric flexure of the Himalayan foreland in Pakistan, in: L. L. Malinconico and R. J. Lillie (eds.), Tectonics of the Western Himalayas, Geological Society of America, Special Paper 232, p. 217-236.

Eittreim, S. L., Hampton, M. A. and Childs, J. R., 1985, Seismic Reflection signature of cretaceous continental breakup on the Wilkes Land Margin, Antarctica, Science, vol. 229, p. 1082-1084.

Farah, A., Lawrence, R. D. and Dejong, K. A., 1982, An overview of the tectonics of Pakistan, in: B. U. Haq and J. D. Milliman (eds.), Marine Geology and Oceanography of Arabian Sea and Coastal Pakistan, p. 161-176.

Folger, D. W., Dillon, W. P., Grow, J. A., Klitgord, K. D. and Schlee, J. S., 1979, Evolution of the Atlantic continental margin of the United States, In: M. Talwani, W. Hay and W. B. F. Ryan (eds.), Deep drilling results in the Atlantic Ocean Continental Margins and Paleoenvironment, American Geophysical Union, Maurice Ewing Series 3, p. 87-108.

Fox, P. J. and Opdyke, N. D., 1973, Geology of the oceanic crust: Magnetic properties of oceanic rocks, Journal of Geophysical Research, vol. 78, no. 23, p. 5139-5154.

Gahagan, L. M. and Ross, M. I., 1987, Phanerozoic plate tectonic reconstructions, Paleoceanographic Mapping Project, Institute for Geophysics, University of Texas, Technical Report No. 90.

Garland, G. D., 1979, Introduction to Geophysics: Mantle, Core and Crust, W. B. Saunders Company, Philadelphia, Pennsylvania, 494 pp.

Gopala Rao, D., 1990, Magnetic studies of basement off the coast of Bombay, West of India, Tectonophysics, vol. 175, p. 317-334.

Grow, J. A., et. al., 1979, The gravity field of the U.S. Atlantic continental margin, Tectonophysics, vol. 59, p. 27-52.

Grow, J. A. and Sheridan, R.E., 1981, Deep structure and evolution of the continental margin off the eastern United States, Ocanol. Acta, Proceeding 26th International Geological Congress, Geology of Continental Margins Symposium, Paris, July 1980, p. 11-19.

Harland, W. B., Cox, A. V. and et. al., 1982, A geological time scale, Cambridge Earth Science Series, Cambridge University Press, Cambridge, 131 pp.

Heezen, B. C. and Tharp, M., 1966, Physiography of the Indian Ocean, Transaction Royal Society London, Series A, vol. 259, p. 137-149.

Heirtzler, J. R., Dickson, G. E., Herron, E. M., Pitman, W. C., and LePichon, X., 1968, Marine magnetic anomalies, geomagnetic field reversals and motion of the ocean floor and continents, Journal of Geophysical Research, vol. 73, p. 2119-2136.

Humayun, M., 1991, Structural Interpretation of the Eastern Sulaiman Fold Belt and Foredeep, Pakistan, M.S. Thesis, Oregon State University, Corvallis, 70 p.

Hutchinson, et. al., 1982, Deep structure and Evolution of the Carolina Trough, in: J. S. Watkins and C. L. Drake (eds.), Studies in Continental Margin Geology, American Association of Petroleum Geologists Memoir 34, p. 129-152.

Jacob, K. H. and Quittmeyer, R. L., 1979, The Makran Region of Pakistan and Iran: Trench-Arc system with active plate subduction, in: A. Farah and A. DeJong (eds.) Geodynamics of Pakistan, Geological Survey of Pakistan, Quetta, p. 305-317.

Jadoon, et. al., 1991, Gravity and Tectonic model across the Sulaiman Fold Belt and the Chaman Fault Zone in western Pakistan-Eastern Afghanistan, Tectonics (in press).

Kaila, K. L., Krishna, U. G. and Tripathi, K. M., 1979, Deep seismic sounding investigations along Mehmadabad-Navsari profile, Cambay basin, National Geophysical Research Institute of India, unpublished report.

Kazmi, A. H., 1979, Active Fault Systems in Pakistan, in: A. Farah and K. A. DeJong (eds.), Geodynamics of Pakistan, Geological Survey of Pakistan, Quetta, p. 285-294.

Keen, C. E., 1982, The continental margins of Eastern Canada: A review, in: R. A. Scrutton (ed.) Dynamics of Passive Margin, Geodynamics Series, vol. 6, p. 45-58.

Khurshid, et. al., 1990, Crustal structure of the Sulaiman Range, Pakistan from gravity data, (Abstract), EOS, Transaction, American Geophysical Union, vol. 71, no. 43, p. 1644.

Klitgord, K. D. and Behrendt, J. C., 1979, Basin structure of the U.S. Atlantic margin, In: J. S. Watkins, L. Montadert and P. Dickerson (eds.), Geological and Geophysical Investigation of Continental Margin, American Association of Petroleum Geologists, Memoir 29, p. 85-112.

Klitgord, K. D. and Grow, J. A., 1980, Jurassic seismic stratigraphy and basement structure of western Atlantic Magnetic Quiet Zone, American Association of Petroleum Geologists Bulletin, vol. 64, no. 10, p. 1658-1680.

Klootwijk, C. G., 1979, A review of paleomagnetic data from Indo-Pakistan fragment of Gondwanaland, in: A. Farah and A. DeJong (eds.), Geodynamics of Pakistan, Pakistan Geological, Survey, p. 41-86.

Kolla, V. and Coumes, F., 1987, Morphology,Internal Structure, Seismic Stratigraphy and Sedimentation of Indus Fan, American Association of Petroleum Geologists, vol. 71, no. 6, p. 650-677.

LaBrecque, J. L., Kent, D. V. and Cande, S. C., 1977, Revised magnetic polarity time scale for Late Cretaceous and Cenozoic time, Geology, vol. 5, p. 330-335.

LePichon, X. and Barbier, F., 1987, Passive margin formation by low-angle faulting within the upper crust: The northern Bay of Biscay Margin, Tectonophysics, vol. 6, no. 2, p. 133-150.

LePichon, X. and Heirtzler, J. R., 1968, Magnetic anomalies in the Indian Ocean and sea-floor spreading, Journal of Geophysical Research, vol. 73, no. 6, p. 2101-2117.

Lillie, R. J., 1991, Evolution of gravity anomalies across collisional mountain belt: Clues to the amount of convergence, Tectonics (in press).

Malinconico, L. L. Jr., 1989, Crustal thickness estimates for the western Himalayas, in: L. L. Malinconico, Jr. and R. J. Lillie (eds.), Tectonics of the western Himalayas, Geological Society of America, Special Paper 232, p. 237-242.

McKenzie, D. P. and Morgan, W. J., 1969, Evolution of triple junction, Nature, vol. 224, p. 125-133.

Merrill, R. T. and McElhinny, M.W., 1983, The earth's magnetic field: its history, origin and planetary perspective, Academic Press Inc., New York, 401 pp.

Moore, G, W. and Eittreim, S. L., 1987, Mechanism of Extension and Rifting at the Antarctica continental margin, Circum-Pacific Council for Energy and Mineral Resources Earth Science Series, vol. 5A, p. 89-97.

Mutter, J. C., Buck, W. R. and Zehnder, C. M., 1988, Convective partial melting 1. A model for the formation of thick basaltic sequences during the initiation of spreading, Journal of Geophysical Research, vol. 93, no. B2, p. 1031-1048.

Nafe, J. E. and Drake, C. L., 1957, Society of Exploration Geophysics, Annual Meeting, 1959, Unpublished paper. The graph referred to is published in: R. E. Sheriff (ed), Encyclopedic Dictionary of Exploration Geophysics, Society of Exploration Geophysicists, 2nd Ed., 1984, p.164.

Naini, B. R., 1980,( Abstract ), A geological and geophysical study of the continental margin of western India and the adjoining Arabian Sea including the Indus Cone, Ph.D Thesis, Columbia University, 182 pp.

Naini, B. R. and Talwani, M., 1983, Structural framework and the evolutionary history of the continental margin of western India, in: J. S. Watkins and C. L. Drake (eds.), Studies in continental margin geology, American Association of Petroleum Geologists, Memoir 34, p. 167-191.

Powell, C. McA., 1979, A speculative tectonic history of Pakistan and surroundings: some constraints from the Indian ocean, in: A. Farah and K. A. Dejong (eds.), Geodynamics of Pakistan, Geological Survey of Pakistan, Quetta, p.5-24.

Quadri, V. N. and Shuaib, S. M., 1986, Hydrocarbon prospects of southern Indus Basin, Pakistan, American Association of Petroleum Geologists, vol. 70, no. 6, p. 730-747.

Quittmeyer, R. C., Farah, A. and Jacob, K. H., 1979, The seismicity of Pakistan and its relation to surface faults, in A. Farah and K. A. DeJong (eds.), Geodynamics of Pakistan , Geological Survey of Pakistan, Quetta, p. 271-284.

Rahman, H., 1963, Geology of petroleum in Pakistan, 6th W.P.C, Frankfurt, Section I, paper 31, PD3, Pakistan.

Raju, A. T. R., 1968, Geologic evolution of Assam and Cambay Tertiary basins of India, American Association of Petroleum Geologists Bulletin, vol. 52, p. 2422-2437.

Raza, H. A., Ahmed, R., Alam, S. and Ali, S. M., 1989, Petroleum zones of Pakistan, Pakistan Journal of Hydrocarbon Research, vol. 1, no. 2, p. 1-19.

Raza, H. A., Ali, S. M. and Ahmed, R., 1990, Petroleum Geology of Kirthar Sub-basin and Part of Kutch Basin, Pakistan Journal of Hydrocarbon Research, vol. 2, no. 1, p. 29-73.

Scrutton, R. A., 1982, Crustal structure and development of sheared passive continental margins, in: R. A. Scruttom (ed.), Dynamics of Passive Margin, Geodynamics series, v. 6, p. 133-140.

Shuaib, S. M., 1982, Geology and Hydrocarbon potential of offshore Indus Basin, Pakistan, American Association of Petroleum Geologists, v. 66, p. 940-946.

Shuey, R. T., Schellinger, D. K., Tripp, A. C. and Alley, L. B., 1977, Curie depth determination from aeromagnetic spectra, Geophysical Journal of Royal Astronomical Society, 50, p. 75-101.

Spector, A. and Grant, F. S., 1970, Statistical models for interpreting aeromagnetic data, Geophysics, vol. 35, no. 2, p. 293-302.

Swift, B. A., et. al., 1987, Subsidence, Crustal Structure, and Thermal Evolution of Georges Bank Basin, American Association of Petroleum Geologists, vol. 71, no. 6, p. 702-718.

Talwani, M. and Heirtzler, J. R., 1964, Computation of magnetic anomalies caused by two-dimensional structures of arbitrary shape, in: Computers in the mineral industries, G. A. Parks (ed.), Stanford University Publication, Geological Sciences, vol. 9, p. 464-480.

Talwani, M., Sutton, G. H. and Worzel, J. L., 1959a, A crustal section across the Puerto Rico Trench, Journal of Geophysical Research, vol. 64, p. 1545-1555.

Talwani, M., Worzel, J. L. and Landisman, M., 1959b, Rapid computation for two-dimensional bodies with application to the Mendocino submarine fracture zone, Journal of Geophysical Research, vol. 64, p. 49-59.

Taylor, P. T., 1968, Interpretation of the North Arabian Sea aeromagnetic survey, Earth and Planetary Science Letter, v. 4, no. 3, p. 232-236.

Udintsev, G. B., 1975, Geological and Geophysical Atlas of the Indian Ocean, Pergamon Press Library of Congress Catalog, no. 76-505517, 151 pp.

Willcox, J. B. and Stagg, H. M. J., 1990, Australia's Southern margin: a product of oblique extension, Tectonophysics, vol. 173, p. 269-281.

Worzel, J. L.,1965, Pendulum gravity measurements at sea 1936-1959, New York, John Wiley and Sons, Inc., 422 pp.

Worzel, J. L. and Shurbet, G. L., 1955, Gravity interpretations from standard oceanic and continental sections, Geological Society of America, Special Paper, no. 62, p. 87-100.

Zuberi, W. A., and Dubois, E. P., 1962, Basin architecture west Pakistan - Symposium of development of Petroleum Resources of Asia and Far East, Tehran.

# APPENDIX

# APPENDIX

## Curie-isotherm Determination

Spector and Grant (1970) have suggested a statistical method for computation of the depth to an ensemble of magnetic sources. Their approach was based on the derivation of Bhattacharyya (1966) who derived an expression for the power spectrum of a single rectangular prism which is buried at a depth h and is of thickness t, length a, width b, and arbitrary magnetization M. This expression for a single prism was later generalized by Spector and Grant (1970) who showed that it can be used to estimate the depth of magnetic bodies using a contour map of magnetic data. A brief description of the results obtained by Spector and Grant (1970) are as follows:

A generalized expression for the spectrum of an ensemble is:

$$\langle E(r,\theta)\rangle = 4\,\Pi^2 k^2 \langle e^{-2hr}\rangle \langle (1-e^{-tr})^2\rangle \langle S^2(r,\theta)\rangle \text{ ----- } 1$$

Equation 1 averaged over $\theta$ reduces the above expression to:

$$\langle E(r)\rangle = 4\,\Pi^2 k^2 \langle e^{-2hr}\rangle \langle (1-e^{-tr})^2\rangle \langle S^2(r)\rangle \text{ ------- } 2$$

where

$$\langle S^2(r)\rangle = 1/\Pi \int_0^{\Pi} \langle S^2(r,\theta)\rangle\, d\theta,$$ the size parameter

$r = (u^2 + v^2)^{1/2}$

$u, v$ = wave number in x and y directions

$\theta$ = arctan (v/u)

$k$ = magnetic moment / unit depth

$r$ = polar wave number

and

for $r < 1/h$

$$< e^{-2hr} > \simeq e^{-2hr}$$

According to Spector and Grant (1970) $e^{-2hr}$ is the dominating factor in equation 2. If the two factors $(1-e^{-tr})^2$ and $S^2(r)$ are removed from equation 2 then,

$$<E(r)> \simeq 4 \Pi^2 k^2 e^{-2hr}$$

and

$$\log <E(r)> \simeq 8 \Pi^2 \log(k) - 2hr$$

as $r = 2 \Pi f$

$$\log <E(f)> \simeq 8 \Pi^2 \log(k) - 4 \Pi h f \quad \text{----------3}$$

This represents an equation of a straight line with slope $4\pi h$ where $8\pi^2 \log(k)$ is a constant. Hence for a plot of $\log<E(f)>$ vs f the slope of a straight line through the data will allow us to calculate the depth of the source. Since equation 3 is a function of frequency (f) only it can be applied to magnetic data along a

profile. The basic assumptions involved in the above approach are:

(i) The magnetic anomaly is due to a real, stationary, and random process.

(ii) The magnetic effect is due to discrete bodies of uniform magnetization which are randomly located.

(iii) The centre of the body has coordinates which are statistically independent of the other body parameters.

(iv) The direction of magnetization of the bodies is approximately parallel to the geomagnetic field direction.

According to Shuey, et. al. (1977) the maximum depth resolvable using the above approach is $L/2\pi$, where L is the length of the longest side of a contour map in a 2-D analysis of Curie depth. For a study of Curie-depth along a profile, L corresponds to the length of the profile.

For the region studied in this thesis the Curie-isotherm should be deeper than 7 km which is the combined thickness of sediment and water. The average depth of the Curie-isotherm along A-A' suggested by the following analysis is about 18 km. The result obtained is dependent on the assumption that there is no significant effect of size and thickness on the magnetic anomalies (i.e. $(1-e^{-tr})^2$ and $S^2(r)$ are negligible). The calculation was done using the software available at the CONMAR. The step by step procedures adopted for Curie-depth analysis in this study are given below.

(i) The magnetic data along profile A-A' (FIG. A1) were resampled for a data spacing of one km. The equally spaced data were then detrended to remove the regional anomaly (FIG. A2).

(ii) The data were then tapered with a cosine square waveform for 10% of the data points. Zeros were then appended to make the total number of data points 512 (FIG. A3).

(iii) A fourier transform was then calculated of the appended data and the power spectrum (E) was estimated. A plot of the Log(E) vs f curve is given in FIG. A4. The slope of a straight line through the data gives the depth of the magnetic source.

(iv) The thirteen data points to the right of the peak in the spectrum (FIG. A4) are approximately on a line. The slope (-224.44) of a line with a least square fit (Gerald and Wheatley, 1984) through these data points suggests an average Curie depth of 18 $\pm$ 1.6 km (FIG. A4)(The variation in the estimated value of the Curie depth is explained below).

The variation of 1.6 km in the estimated value of the Curie-depth (18 km) does not indicate the upper and lower bound for the Curie-depth of the region. The value only indicates the variation in the estimated value one may expect by fitting lines with different slopes through the data points.

FIG. A4 also suggests that beyond the frequency of 0.2 c/km the signal-to-noise ratio is very low and the spectrum is noisy. This noise is also present in the part of the spectrum of frequency

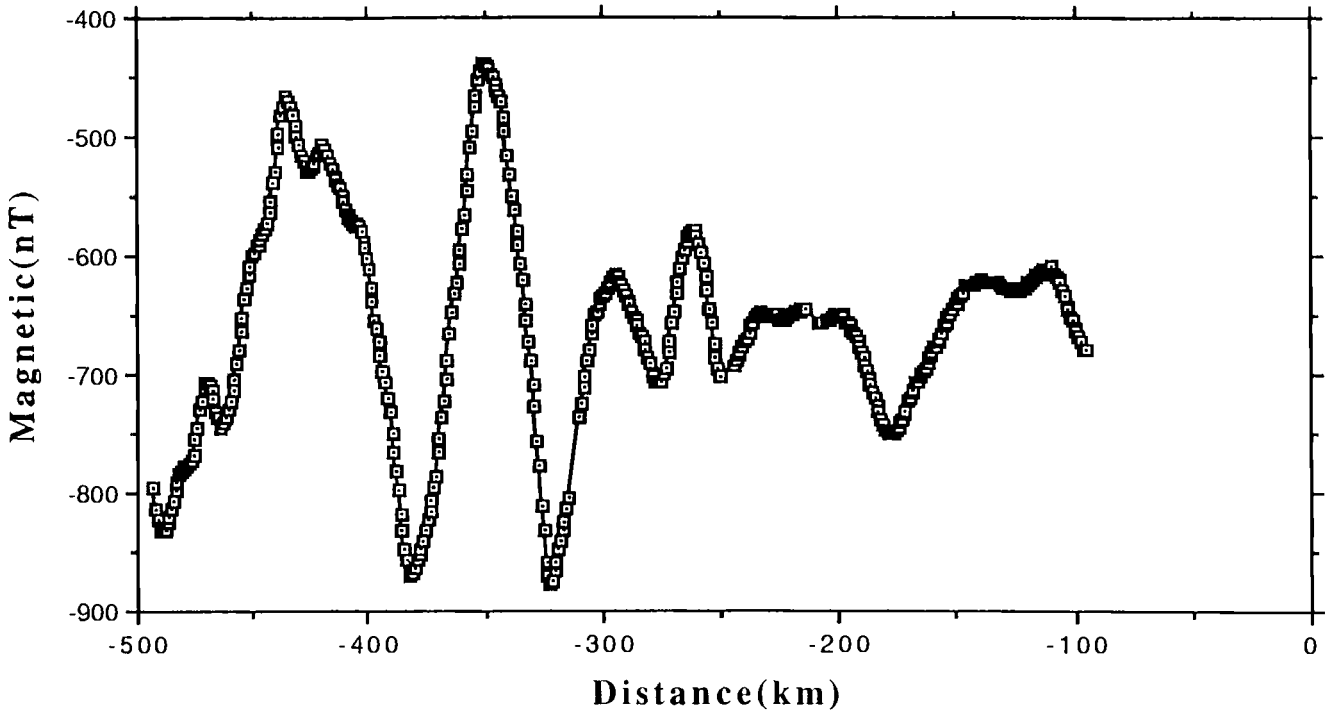


FIG. A1 Magnetic data along profile A-A'.

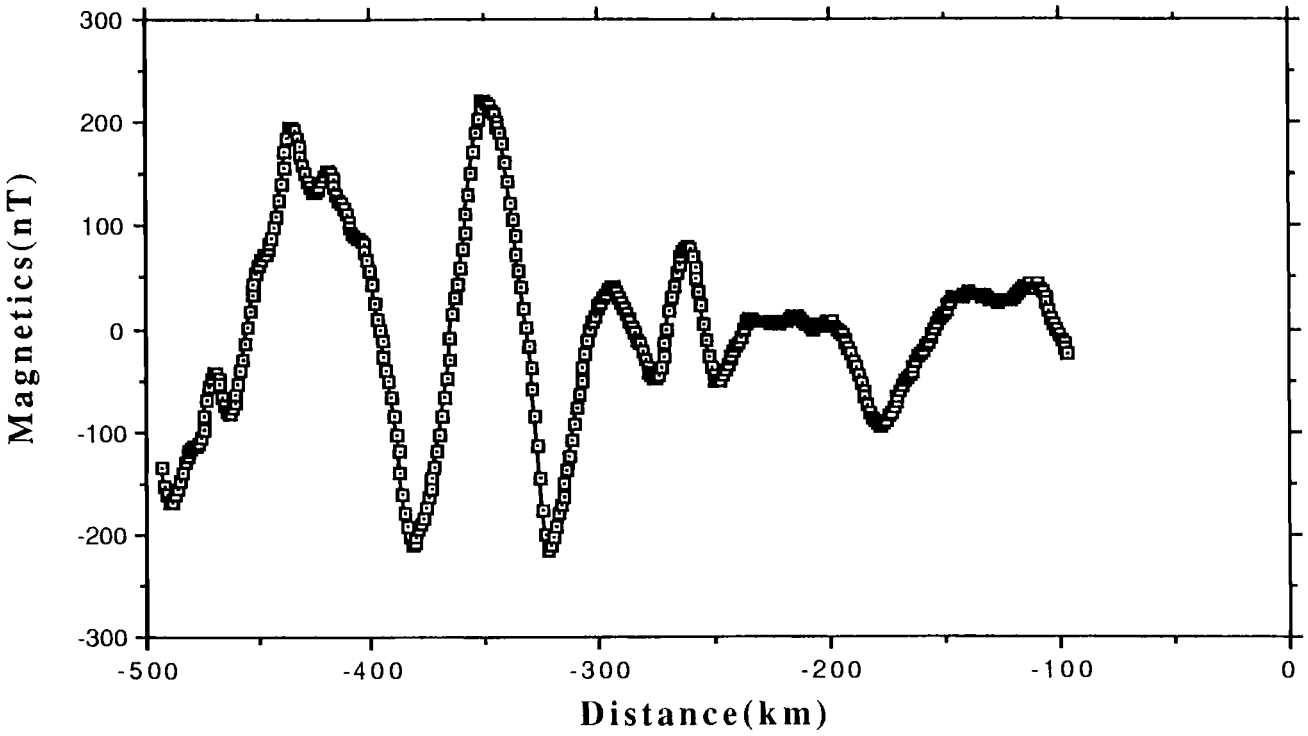


FIG. A2 Equally spaced and detrended magnetic data.

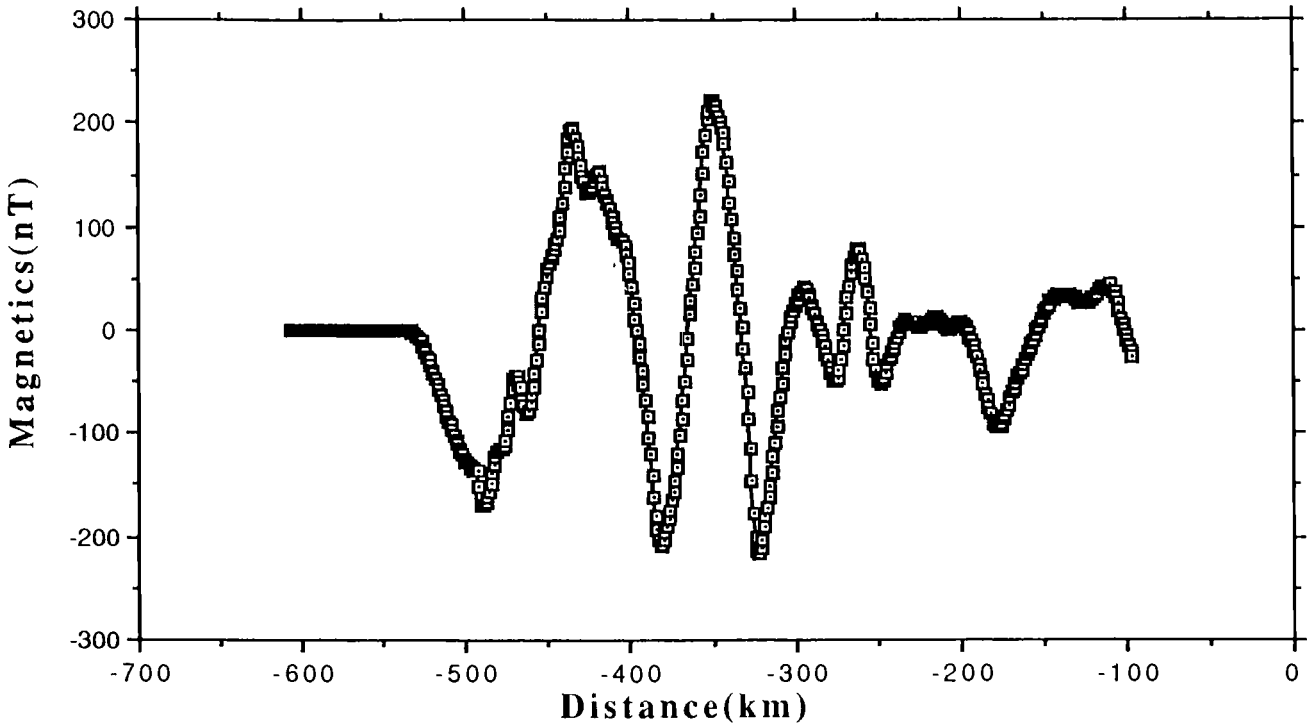


FIG. A3 Tapered and appended magnetic data.

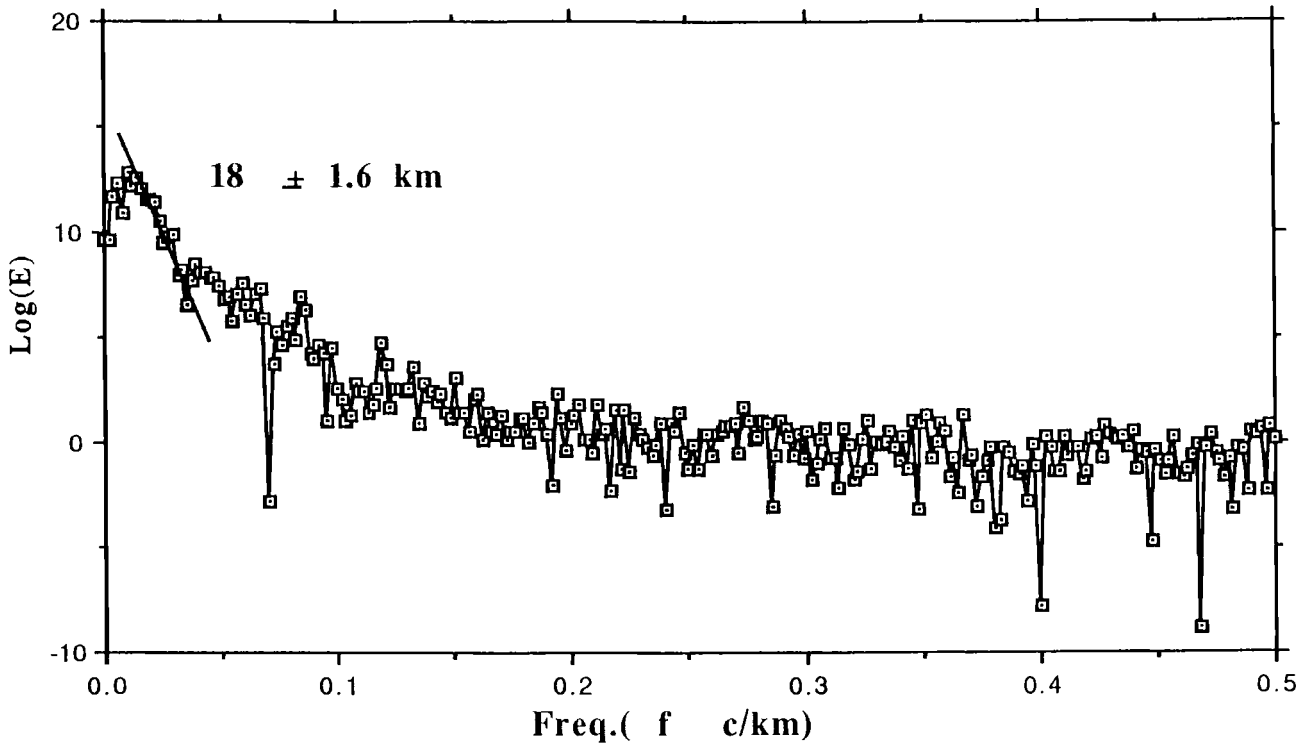


FIG. A4 Spectrum of the magnetic data along profile A-A'. The estimated value of the Curie-depth is 18 ± 1.6 km. The variation of ± 1.6 km does not represents the upper and lower bound for the Curie-depth of the region. It only represents the possible variation in the slope of the lines that can be fitted through the data.

less than 0.2 c/km but in this part the signal-to-noise ratio is very high. The noise in the data is due to instrument error, navigational error and noise in the magnetic field. The instrument and navigation errors can be minimized by careful operation of the instrument and careful recording of the ships position during the survey. As the data I used was prerecorded I did not have any control on the instrumental and navigational errors. The noise in the magnetic field however, cannot be avoided but the error in the data due to this noise can be reduced by correlating the data with the data recorded during a noise-free period. As I did not have access to any noise-free data it was not possible to check for noise in the field.

A complete description of the above method for the determination of Curie-depth as applied to magnetic data can be seen in Connard (1980) and Foote (1986).

# REFERENCES

Bhattacharyya, B. K., 1966, Continuous spectrum of the total-magnetic-field anomaly due to a rectangular prismatic body, Geophysics, vol. 31, no. 1, p. 97-121.

Connard, G. G., 1980, Analysis of aeromagnetic measurements from the Central Oregon Cascades, M.S. Thesis, Oregon State University, Corvallis, Oregon, 101 pp.

Foote, R. W., 1986, Curie-point isotherm mapping and interpretation from aeromagnetic measurements in the Northern Oregon Cascades, M.S. Thesis, Oregon State University, Corvallis, Oregon, 115 pp.

Gerald, C. F. and Wheatley, O. P., 1984, Applied Numerical Analysis, Addison-Wesley Publishing Company Inc., Menlo Park, California, 579 pp.

Shuey, R. T., Schellinger, D. K., Tripp, A. C. and Alley, L. B., 1977, Curie-depth determination from aeromagnetic spectra, Geophys. Journal of Royal Astronomical Society, vol. 50, p. 75-101.

Spector, A. and Grant, F. S., 1970, Statistical Models for interpreting aeromagnetic data, Geophysics, vol. 35, no. 2, p. 293-302.